Title
The Effects of the Postmortem Interval on the Alzheimer's Disease Metabolome

Author
Sylvestre, Duncan

Publication Date
2021

Peer reviewed|Thesis/dissertation

The Effects of the Postmortem Interval on the Alzheimer's Disease Metabolome

By

DUNCAN SYLVESTRE
THESIS

Submitted in partial satisfaction of the requirements for the degree of

MASTER OF SCIENCE

in

Nutritional Biology

in the

OFFICE OF GRADUATE STUDIES

of the

UNIVERSITY OF CALIFORNIA

DAVIS

Approved:

Ameer Taha, Chair

Jon Ramsey

Brittany Dugger

Committee in Charge

2021

Table of Contents

Acknowledgements

To my mentor, Dr. Ameer Taha, thank you for all the time that you spent mentoring me. I learned a lot not only about analytical chemistry but also about scientific writing. I'm forever grateful to have had the opportunity to have worked with you.

I would like to thank my thesis committee member Dr. Brittany Dugger for time spent providing feedback for my thesis and for the open scope sessions. I learned a lot about pathology and neuroanatomy in a way that a textbook could never compare. Similarly, I'd like to thank my other thesis committee member Dr. Jon Ramsey for taking the time to read and provide in-depth feedback for my thesis. It has been greatly improved by your feedback.

I would also like to thank Dr. Danielle Harvey for her invaluable help interpreting the statistical analysis that we performed for Study 2.

I would also like to thank Dr. Slupsky for supporting me all these years, for giving me feedback to help improve my writing. Without you I would never have had the opportunity to study at UC Davis.

Finally, thank you everyone from the Slupsky and Taha labs for your support over the past six years.

Abstract

Evaluating the effects of postmortem ischemia on brain metabolites has been a longstanding challenge in *ex vivo* metabolomic studies. This thesis sought to first evaluate which metabolites are affected by short-term postmortem ischemia in rats, through the use of head-focused microwave irradiation as a control group to one group receiving CO_2-induced hypercapnia/ischemia with microwave irradiation, one group receiving CO_2 and microwave irradiation with a postmortem interval simulating a typical dissection time, and one group receiving CO_2 only (Study 1). The subsequent objective was to take the postmortem interval into account in an evaluation of metabolites in postmortem prefrontal cortex taken from AD patients and control patients, both with and without a cerebrovascular disease (CeVD) diagnosis (Study 2). CeVD represents a state of chronic ischemia potentially discernable from acute postmortem ischemia, which could manifest in metabolomic differences between AD and CeVD. Study 1 demonstrated substantial postmortem changes in brain energy and glycosylation pathways, as well as levels of amino acids, nucleotides, neurotransmitters, lipids, and antioxidants as a result of both ischemia and brain dissection, compared to controls subjected to head-focused microwave irradiation. Study 2 found that compared to controls without CeVD, AD patients without CeVD had reduced levels of fumarate, glutathione, and sarcosine, while α-hydroxybutyrate was confounded by age and postmortem interval in AD subjects without CeVD. This thesis demonstrates that postmortem ischemia should be considered as an important variable in postmortem brain metabolomic studies, to better determine metabolite changes that are potentially masked by the postmortem interval, especially with co-occurring vascular disease pathologies.

Introduction

Alzheimer's Disease (AD) is a progressive, irreversible neurodegenerative disorder that causes cognitive impairment, disability, and ultimately death[1]. AD affects approximately 6 million people in the US and 24 million people worldwide[2,3]. It is clinically the most common form of dementia, defined as a syndrome in which there is a deterioration in memory, thinking, behavior, and the ability to perform everyday activities[4]. At present, there is no treatment for AD that can halt or reverse progression.

AD is characterized by the postmortem presence of β-amyloid plaques and deposits of hyperphosphorylated tau proteins in the form of neurofibrillary tangles (NFTs). These pathologies have been associated with synaptic loss in multiple areas of the brain[5]. There is also postmortem evidence of astrocytosis[1,6] and gliosis[7], suggestive of inflammation.

Clinically, AD is associated with dementia. However, there are other forms of dementia that produce similar symptoms that complicate diagnoses[8]. The gold standard of AD diagnosis – the presence of plaques and NFTs in select neuroanatomic regions – can only be confirmed after death through an autopsy[9]. One study showed that 25% of patients received a clinical diagnosis of "probable AD" using clinical dementia ratings, manifested inconsistent AD diagnosis postmortem, while 64% of AD diagnoses presented mixed pathologies including coexisting vascular disease or Parkinson's disease[10].

Pathological diagnosis of AD:

Postmortem diagnosis of AD is evaluated on three scales: the Aβ plaque score, evaluated with Thal Aβ phase (TAP) scoring[11], NFT progression, evaluated through Braak scores[6], and CERAD scores, which evaluate the presence of neuritic plaques[12]. Braak staging progresses from scores of one to six evaluating the neuroanatomic location of NFT deposits. Initially, at stage I or II, isolated to moderate tangles appear in pyramidal cells in the hippocampus, transentorhinal

cortex and the antero-dorsal nucleus. It then progresses throughout the hippocampus and cortex, as well as appearing in the amygdala, basal magnocellular complex, and hypothalamus in stage III and IV, before becoming systemically present in all cortical and subcortical regions of the brain at moderate to large abundance (stages V and VI)[6].

CERAD uses a semi-quantitative assessment of neuritic plaques, defined as plaques that contain abnormal neuronal processes, including both Aβ and NFTs[13], ranging from a score of "none" to "frequent"[12],while TAP uses a hierarchical distribution of immunohistochemistry (IHC) positive Aβ plaques ranging from a score of "none" to a score of 5, in which Aβ deposits found in the neocortex, allocortex, diencephalon, brain stem, and cerebellum are recorded as a measure of location rather than severity[11]. The main difference between CERAD and TAP is that CERAD specifically measures neuritic plaques in the neocortex only, while TAP is scored based on the neuroanatomic location of any Aβ plaque. CERAD also only evaluates the entorhinal cortex, midfrontal cortex, middle temporal cortex, and inferior parietal cortex using a modified Bielschowsky silver stain. CERAD evaluation of neuritic plaques can also use IHC[14,15] when available, however, as silver staining requires a well-trained technician and is influenced by ambient temperature[12]. TAP, on the other hand, uses IHC with antibodies specific to Aβ, which is a more sensitive method for detecting plaques. However, the specificity of TAP has been called into question, as some studies have found that there is no strong correlation between the presence of Aβ plaques in the various regions of the brain evaluated by TAP and clinical symptoms of dementia[16].

Proposed causes of AD:

Knowing the underlying pathophysiology of AD is paramount to developing effective treatments which are currently lacking. Multiple pathways have been proposed[17-26]. These

include beta-amyloid (Aβ) accumulation[21], formation of phosphorylated tau[22], inflammation associated with astrocytosis and microglial activation[20,24], disturbances in monoamine neurotransmitter metabolism[23,25,26] and energy deficits[21,27].

The "Amyloid-β Hypothesis" argues that the buildup of Aβ plaques is the root cause of AD[21]. The "Tau Hypothesis" argues the same for the buildup of NFTs. Both hypotheses have had significant academic support for decades[22].

Plaques are formed through the aggregation of amyloid-β (Aβ), derived from the amyloid precursor protein (APP) cleaved by beta- and gamma-secretase, of which some oligomers have been shown to disrupt synaptic function and therefore affect memory in transgenic mice[21]. The gene that encodes for gamma-secretase (which cleaves amyloid precursor protein to produce Aβ fragments[28]) is located on chromosome 21, and patients with trisomy 21 exhibit AD-like disorders at ages as young as 40[29]. While correlations between Aβ accumulation and AD progression are strong, there is no clear evidence that Aβ accumulation is a direct cause of AD[30]; it is a distinct possibility that Aβ accumulation may promote neurodegeneration through stimulation of inflammatory pathways.

Further support for the β-Amyloid hypothesis stems from transgenic animal studies[31]. For instance, mutations in APP have been shown to lead to plaques in the brain and to cognitive impairment in mice[19]. This mouse model substitutes the valine at residue 717 of APP for a phenylalanine, and progressively develops the pathological hallmarks of AD, including Aβ deposits, synaptic loss, astrocytosis, and microgliosis. Additional mouse models have overexpressed human APP transgenes, and have exhibited age dependent amyloid deposition with gliosis and dystrophic neurites[32]. Yet others have exhibited elevated levels of Aβ42 without any plaque pathology[33]. A major drawback of these models, however, is that they only

recapitulate a portion of the disease pathology. APP transgenic mice, for example, do not present tau pathology, and combine several mutations that do not normally co-occur in AD to generate Aβ deposits[34].

NFTs form when tau, a protein associated with microtubules, becomes hyperphosphorylated, causing it to form insoluble aggregates[22] that interfere with microtubule dependent traffic[35]. Some studies have found that these tangles (also known as NFTs) are much more strongly associated with the duration and severity of AD compared to Aβ plaques[36]. NFTs have been shown to lead to the dissolution of microtubules, ultimately leading to a decline in axonal and dendritic transport and impaired trafficking of proteins through the endoplasmic reticulum and Golgi body[5,35]. Like with Aβ, tauopathies have been linked with specific mutations, though in this case it is a collection of mutations in the gene coding the tau protein collectively referred to as FTDP-17[37,38].

To date, the majority of transgenic animal models that have resulted in phenotypic manifestations of human tauopathies have been in mice[39]. While ordinarily, the adult mouse homolog of tau is spliced into 4R isoforms, human tau is spliced into six isoforms evenly distributed between 3R and 4R forms[40]. Despite this, a transgenic model that demonstrated human-like pathology, with insoluble hyperphosphorylated tau and argyrophilic intraneuronal inclusions composed of tau-immunoreactive filaments, was eventually developed[41]. Debate remains, however, as to whether or not tau is protective or pathological. Tau laden neurons have been demonstrated to be able to live for decades[42], and neuronal loss is correlated with, but greatly exceeds NFT formation[43]. One possible reason for this observation is that NFTs could be a cellular response to oxidative stress[44]. It is more likely to be pathological, however, as mutant tau induces faster misfolding than tau found in sporadic AD patients[45].

Despite significant research focus, drugs that target beta-amyloid and phosphorylated tau accumulation have shown no clinically significant results on dementia symptoms[46,47]. For instance, aducanumab, an IgG1 monoclonal antibody that targets Aβ protein aggregates was halted in phase 3 clinical trials because AD patients showed no difference in the Clinical Dementia Rating Sum of Boxes (CDR-SB) scale, or the secondary measures of the Mini-Mental State Exam (MMSE) relative to a placebo[48]. Similarly, solanezumab[46] and gantenerumab[47], both monoclonal antibodies targeting Aβ like aducanumab, have had no efficacy in reducing clinical dementia ratings on the Alzheimer's Disease Assessment Scale (ADAS-cog14). CDK5 inhibitors targeting aberrant tau such as roscovitine have been demonstrated to reduce NFTs in mouse models[49], but clinical trials in humans have resulted in no effect on disease progression[50]. One possible reason for this could be that these studies measured two different outcomes; many animal models use physiological markers for disease severity, such as presence of NFTs or Aβ plaques, while clinical trials in humans measure outcomes on clinical dementia scales.

AD is associated with activated microglia in response to the formation of Aβ plaques[24]. Microglia driven responses release pro-inflammatory cytokines[20,24], which recruit astrocytes that further enhance the inflammatory response[18]. Cytokine signaling is coupled to cyclooxegenase-2 and lipoxygenase enzymes which convert polyunsaturated fatty acids into pro-inflammatory eicosanoids that exacerbate brain inflammation[51,52]. These factors can both in isolation and synergistically contribute to cellular dysfunction and death[53,54].

The cholinergic system is considered one of the most impacted neurotransmitter systems in AD[55]. Several studies have shown that anticholinergic drugs in healthy subjects have an amnestic effect and induce memory deficits comparable to those in elderly subjects without dementia[56]. A specific cholinergic deficit involving the nucleus basalis magnocellularis of

Meynert, cortex and hippocampus was consistently identified in postmortem brain samples from Alzheimer's patients compared to controls not diagnosed with dementia[57]. Thus, acetylcholinesterase inhibitors are approved by the Food and Drug Administration (FDA) for delaying early symptoms of memory decline in individuals with dementia, although their use does not prevent or cure AD[58].

The glutamatergic system has also been implicated in AD[59,60]. Glutamate is released into the synaptic cleft, triggering potentiation in an adjacent neuron[17]. Glutamate is then taken up by astrocytes through excitatory amino acid transporter 1 and 2, the latter of which is responsible for as much as 95% of all glutamate transport in astrocytes[61] and its loss has been observed in AD patients[62]. Ionotropic glutamate receptors, notably N-methyl-D-aspartate (NMDA) have been implicated in cognitive deficits related to AD[63] leading to FDA-approval of anti-glutamatergic drugs (e.g. memantine) for delaying symptoms of early-onset dementia[64].

Disruption of other monoamine neurotransmitter systems has been implicated in AD[23,25,26]. Some authors have reported reduced cerebrospinal fluid (CSF) concentrations of serotonin[26] and dopamine[23,25], possibly suggesting some systemic damage of monoaminergic neurons. The concentrations of their downstream metabolites, homovanilic acid, and dihydroxyphenylacetic acid have been observed to decrease significantly in the cerebrospinal fluid of AD patients with severe mental deterioriation[65,66] but not in patients with more mild symptoms[26,66,67], potentially suggesting decreased monoamine neurotransmitter turnover is a contributing factor to the disease. However, this change in monoaminergic neurotransmitters is also likely the consequence of depression, which is present in as much as 50% of AD patients, especially those with severe cognitive impairment[68]. Pharmacological interventions targeting monoamine neurotransmitters, such as sertraline, have shown minimal or no efficacy in delaying

cognitive impairment or treating depression concurrent with AD [69]. Further, some studies have found that antidepressant use is associated with a greater risk of cognitive impairment[70].

Heterogeneity in AD

AD is a heterogeneous brain disorder. It has been evaluated that while clinical AD diagnoses are accurate in 86-90% of cases, in roughly 36% of cases, at least one additional neuropathologic diagnosis is present, of which cerebrovascular disease (CeVD), is the most common, while Lewy Body Disease and Frontotemporal lobar degeneration (FTD) are less so[71,72]. CeVD is a broad classification of conditions, such as large vessel disease and small vessel disease, in which cerebral blood flow is restricted, leading to chronic ischemia, neuronal death, and cognitive impairment[73]. Lewy Body Disease results from the buildup Lewy bodies derived from alpha-synuclein aggregation within neurons and FTD is characterized by the atrophy of the frontotemporal lobe due to TDP-43 accumulation[74], or alternatively with tauopathies[75] or ubiquitin[76].

CeVD is associated with a 12-fold increased risk of AD dementia, as both AD and CeVD share many common risk factors, such as the APOE ε4 genotype[77] and atrial fibrillation[78]. Vascular risk factors have been linked to progression from mild cognitive impairment to full AD[79]. However, results are mixed, and other studies have found a lack of association between vascular risk factors and AD specifically[80].

CeVD is typically associated with subcortical white matter hyperintensities (WMH) that appear on T2-weighted MRI scans, and their presence is associated with a reduction in cerebral blood flow, leading to significant ischemia and associated impairment in primarily executive function, and to a lesser extent attention, memory, and social cognition[81]. Further, ischemia is the most common cause of stroke, being responsible for approximately 80% of all strokes[82]. The

other form of stroke, hemorrhagic stroke, is characterized by bleeding in the brain due to the rupture of a blood vessel and is associated with high mortality[3]. CeVD can alternatively manifest in more sudden vascular insufficiency associated with stroke, which often leads to cognitive impairment[83]. While both WMH and ischemic stroke lead to axonal loss through Wallarian degeneration[84] in which affected axons break apart and are infiltrated by macrophages, the main difference between the two is that the more common subcortical form manifests as chronic low-grade ischemia whereas the ischemic type is secondary to an infarct within cerebral arterioles[85].

Postmortem, CeVD has multiple diagnostic criteria[86-88]. One such criteria creates a composite lesion score by evaluating the presence of large infarcts, lacunes (empty spaces), and leukoencephalopathy[88]. Another divides vascular dementia pathology into six subtypes: the presence of either a single large infarct, or several small infarcts summing to a total of 50mL tissue loss (type I), the presence of multiple small or microinfarcts (type II), the presence of strategic infarcts in the thalamus or hippocampus (type III), cerebral hypoperfusion such as due to hippocampal sclerosis, or ischemic damage (type IV), evidence of cerebral hemorrhages (type V), or cerebral vascular changes with AD pathology (type VI)[87]. A third criteria creates a staging system beginning with vessel wall modifications (such as through arteriosclerosis and amyloid angiopathy), progressing through perivascular and white matter modifications, to cortical microinfarcts culminating in large infarcts within the cortex[86].

The two main pathologies that are considered to contribute to cognitive impairment associated with CeVD are arteriosclerosis and cerebral amyloid angiopathy (CAA). Arteriosclerosis typically manifests in the loss of smooth muscle cells from the tunica media concurrent with deposits of fibro-hyaline material, resulting in the narrowing of the lumen and thickening of the vessel wall[85]. Arteriosclerosis is evaluated semi-quantitatively with categories

corresponding to “none” (representing no arteriosclerosis), "mild” (in which there is mild thickening of the vessel media and mild fibrosis), “moderate” (in which there is partial loss of smooth muscle cells and moderate hyaline fibrosis) and “severe” in which smooth muscle is completely lost coupled with severe hyaline fibrosis and stenosis of the lumen[89]. CAA is conversely characterized by the accumulation of Aβprotein on the walls of small to medium sized arteries and arterioles in leptomeninges and the cortex[90]. These accumulations appear green under polarized light when stained with Congo Red and fluoresce under ultraviolet light or when stained with thioflavin S. Diagnosis is further complicated, however as it frequently manifests in AD as well[91].

Metabolomics to understand defective pathways in AD:

In view of the complexity and heterogeneity of AD, a detailed analysis of multiple underlying pathways impacted by the disease is warranted, particularly in individuals with CeVD. Metabolomics, using ^{1}H Nuclear Magnetic Resonance (NMR) spectroscopy is one way of comprehensively evaluating changes in inter-linked pathways, as it allows for the simultaneous measurement of dozens of compounds involved in brain energy utilization, lipid, carbohydrate and amino acid metabolism, and neurotransmitter and protein turnover.

NMR is performed by using a large magnet to align all of the individual dipoles within a sample, thereby magnetizing it, and then using a burst of radio frequency energy to tip those dipoles into a plane perpendicular to the ground magnetic field. The procession of protons as they return to their lower energy ground state can be captured as the free induction decay, to identify atoms and synthesize molecular structures involved[92]. Protons within different structures will process at different frequencies, which appear as distinct peaks when the spectrum is Fourier transformed[92].

NMR analysis is untargeted but quantitative. This means that compounds detected above the baseline noise can be identified and quantified against an internal standard added to the sample, to obtain absolute concentrations. A representative NMR profile of a rat brain sample is shown in **Figure 1**. As shown, the postmortem rat brain spectrum is high in lactate (labelled with the letter A), creatine (labelled with the letter B), glutamate (labelled with the letter C), and *myo*-inositol (labelled with the letter D). While **Figure 1** shows a spectrum of whole rat brain, regional analysis has indicated variation in only some metabolites, such as inositol, which is higher in the cerebellum compared to the cortex[93]. There are also differences in metabolite concentrations between organs. For instance, neurotransmitters such as glutamate are significantly lower in peripheral organ systems such as the liver, compared to the brain [94].

Prior studies that have used mass-spectrometry analysis have found that choline, GABA, and N-Acetylaspartate are decreased in the Inferior Temporal Gyrus (ITG) in AD relative to controls, while cysteine and reduced glutathione are increased[95]. Further, choline, GABA, and N-Acetylaspartate were negatively correlated with Braak NFT and CERAD scores while cysteine, reduced glutathione, and spermidine were positively with those same measures of disease severity[95]. Additionally, Braak NFT and CERAD scores have also been found to correlate with postmortem brain glucose concentrations, as well as levels of the glucose transporter GLUT3 in humans[27].

The postmortem problem in human research

A current gap in knowledge is that no study has investigated the profile of human brain metabolites that could be involved in cognitive impairment in patients with or without CeVD. However, measuring metabolites in postmortem brain samples is complicated in both humans and animal models by the fact that the concentrations of these metabolites are often disrupted by

the global ischemia that happens during the agonal state shortly before death, death itself, and the subsequent postmortem interval (PMI)[96-98]. Postmortem ischemia caused by the halting of blood flow to the brain (i.e. reduced glucose and oxygen), is associated with the rapid release of glutamate into synapses, resulting in post-synaptic release of extracellular calcium, fatty acids and excitatory neurotransmitters[99,100].

In animal models, conclusively identifying affected pathways requires euthanasia techniques such as head-focused microwave irradiation, to avoid ischemia-induced metabolic changes that happen during death. Microwave irradiation involves the channeling of a 6-14 kW beam of microwave energy to the head of a restrained animal[97,101]. The interaction of the microwave with the brain's water content, increases in the brain's internal temperature to 70-80°C[102], thus inactivating enzymes. This approach has been shown to be effective in measuring brain ATP and acetylcholine concentrations in rats, which otherwise decrease to non-detectable levels during postmortem ischemia[103,104].

The process of brain dissection further complicates measurement of metabolites in postmortem tissue, a problem which microwave irradiation neatly sidesteps. While the effects of brain dissection on brain energy metabolites such as ATP are understudied, its effects of dissection on oxidized lipid metabolites have been shown[101,105].

The problem of postmortem ischemia and brain dissection cannot be evaded in human brain research. However, one can lean on rodent models to identify metabolites that could be affected by postmortem ischemia and / or brain dissection, and are thus unreliable. To date, the effects of postmortem ischemia on the brain have been limited to a few metabolites in rodents. For instance, Veech et al.[98] showed that ATP and acetylcholine concentrations measured postmortem reflect *in vivo* concentrations when postmortem enzymatic activity is quickly

inhibited either through a “freeze-blowing” technique or through microwave irradiation.[98]. To my knowledge, no study has looked at the effects of postmortem brain dissection on metabolite levels. Thus, a thorough investigation on the impact of postmortem ischemia and dissection on the entire brain metabolome is needed to better interpret postmortem human brain data.

Thesis hypothesis and objectives:

The overall hypothesis of my thesis is that changes associated with the postmortem interval (e.g. ischemia and brain dissection) alter metabolomic profiles of AD through changes in energy and neurotransmitter homeostasis**.** The hypothesis is based on 1) rodent studies showing that postmortem ischemia alters multiple brain metabolites such as ATP and acetylcholine[96,98,106-108] and 2) studies showing changes in these pathways in postmortem AD brain compared to pathologically normal controls[109]. Additionally, the contribution of postmortem ischemia and CeVD to previously reported changes in AD has not been investigated. Postmortem ischemia is a relatively acute state of reduced blood flow to the brain, compared to CeVD in which blood flow to several areas of the brain may be restricted chronically due to blood vessel damage. Thus, the overall goal of my thesis is to dissect both factors to understand how each may contribute to metabolomic changes in AD. Because CeVD is difficult to model in animals, I will focus on characterizing the effects of postmortem ischemia and dissection on the rat brain metabolome. I will then include the postmortem interval as a confounder in my metabolomics analysis of postmortem AD and non-AD brains with or without CeVD, to determine whether AD and CeVD have dissociable metabolomic signatures.

The specific thesis aims are as follows:

1) Determine the effects of postmortem ischemia and brain dissection on the rat brain metabolome using NMR; and

2) Use this knowledge to determine the effects of AD with or without concurrent CeVD on postmortem prefrontal cortex brain metabolites, as a first step towards identifying dissociable pathways underlying AD and CeVD.

In Aim 1, ischemia was induced in rats using CO_2 asphyxiation for 2 to 6.4 minutes and compared to rats subjected to head-focused microwave irradiation. Brain dissections were also performed in microwave-irradiated and non-irradiated rats. Brain metabolites were measured in whole brain (versus regional analysis), to obtain detectable signals for a broad range of molecules on NMR.

Aim 2 investigated metabolomic signatures in post-mortem pre-frontal cortex of control and AD patients with or without CeVD. Pre-frontal cortex was chosen due to the presence of plaques and NFTs during the advanced phases of the disease[6].

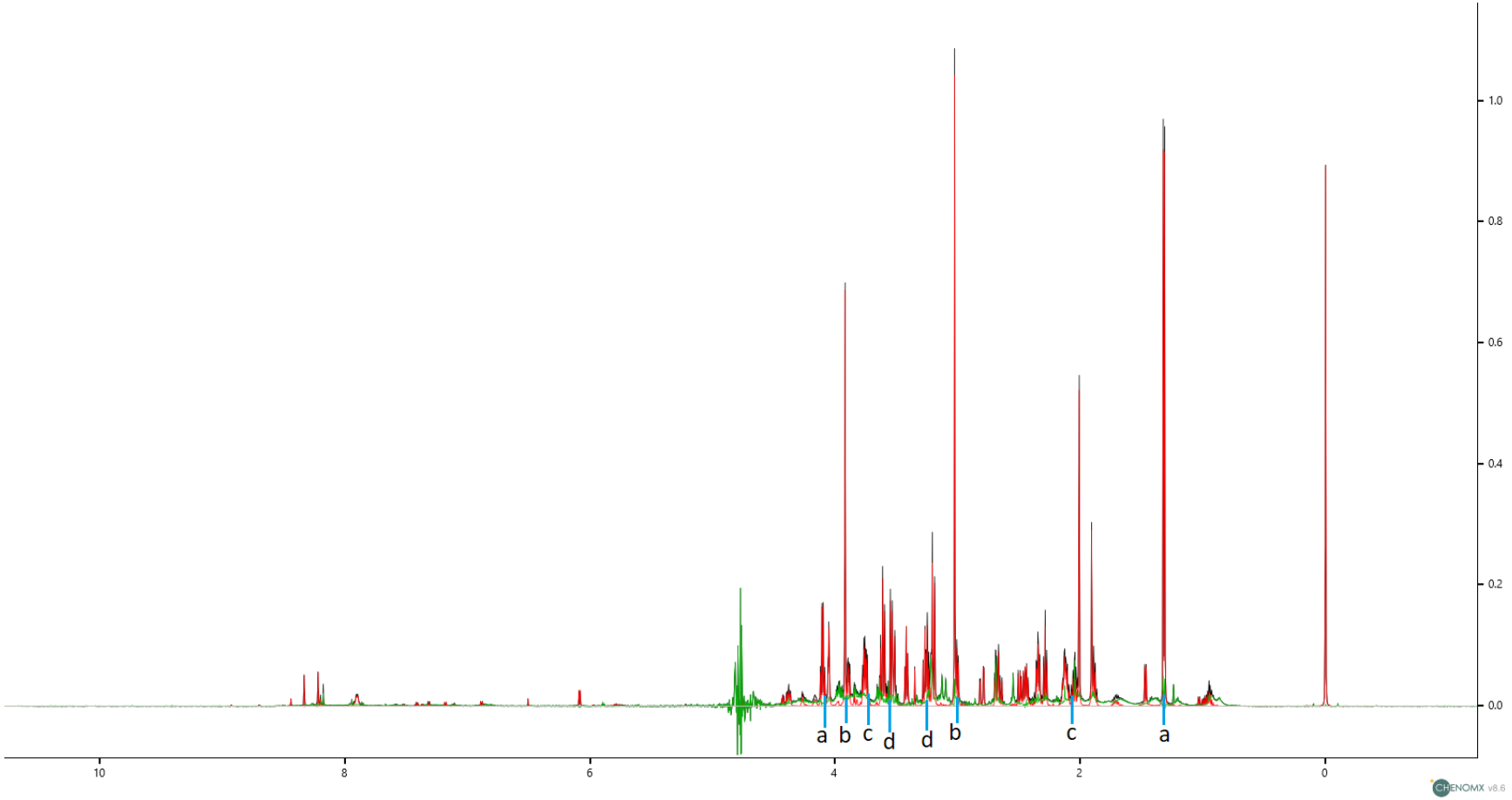

Figure 1: Partially Annotated normal adult Rat Brain NMR Spectrum. Here, the peaks for lactate (a), creatine (b), glutamate (c), and *myo*-inositol (d) are labeled. A total of 62 metabolites were identified and quantified in this spectrum. The x-axis represents the ppm shift of the Fourier transformed spectrum, while the y-axis represents the relative intensity compared to a reference standard of DSS-d6. Each compound has multiple labeled peaks, each of which corresponds to a different proton in the structure of the compound.

Effects of hypercapnia / ischemia and dissection on the rat brain metabolome

Duncan A. Sylvestre[1,2], Yurika Otoki[1,3], Adam H. Metherel[4], Richard P. Bazinet[4], Carolyn M. Slupsky[1,2], and Ameer Y. Taha[1,5,*]

[1] Department of Food Science and Technology, University of California, Davis
[2] Department of Nutrition, University of California, Davis
[3] Food and Biodynamic Laboratory, Graduate School of Agricultural Science, Tohoku University, Sendai, Miyagi, Japan
[4] Department of Nutritional Sciences, University of Toronto, ON, M5S 1A8, Canada
[5]West Coast Metabolomics Center, Genome Center, University of California, Davis

*To whom correspondence should be addressed.
Ameer Y. Taha
Department of Food Science and Technology, College of Agriculture and Environmental Sciences, University of California Davis, One Shields Avenue, Davis, CA, USA 95616
Phone: (+1) 530-752-7096; Email: ataha@ucdavis.edu

Keywords: Metabolomics; Ischemia; Microwave Fixation; Irradiation; Dissection

Running Title: Hypercapnia/Ischemia and dissection alter brain metabolite concentrations

Abbreviations List

- ATP: Adenosine Triphosphate
- BHT: Butylated hydroxytoluene
- DSS-d6: d6-4,4-Dimethyl-4-silapentane-1-sulfonic acid
- EDTA: Ethylenediaminetetraacetic acid
- GABA: gamma-aminobutyric acid
- MW: Microwave Irradiation
- NOESY: Nuclear Overhauser Effect Spectroscopy
- NMR: Nuclear Magnetic Resonance
- PCA: Principal Component Analysis

Abstract

It is known that brain energy metabolites such as ATP are quickly depleted during postmortem ischemia; however, a comprehensive assessment on the effects of preceding hypercapnia/ischemia and the dissection process on the larger brain metabolome remains lacking. This study sought to determine aqueous metabolites impacted by ischemia (which is preceded by hypercapnia) and brain dissection using Nuclear Magnetic Resonance. Metabolites were measured in rats subjected to 1) head-focused microwave irradiation (control group); 2) CO_2–induced hypercapnia/ischemia followed by immediate microwave irradiation; 3) CO_2 followed by decapitation and then microwave irradiation 6.4 minutes later, to simulate a postmortem interval equivalent to typical dissection times; and 4) CO_2–induced hypercapnia/ischemia followed by dissection within 6.4 minutes (no microwave fixation) to test the effects of brain dissection on the metabolome. Compared to microwave-irradiation as the sole treatment (the control group), concentrations of high-energy phosphate metabolites and glucose were significantly reduced, while β-hydroxybutyrate and lactate were increased in rats subjected to all other treatments. Several amino acids and neurotransmitters (glutamate and GABA) increased. Sugar donors involved in glycosylation decreased and nucleotides decreased or increased following hypercapnia/dissection and dissection. sn-Glycero-3-phosphocholine decreased and choline increased, indicating postmortem changes in lipid turnover. Antioxidants increased following hypercapnia/ischemia but decreased to control (i.e. microwave-irradiation) levels following dissection. This study demonstrates substantial post-mortem changes in brain energy and glycosylation pathways, as well as protein, nucleotide, neurotransmitter, lipid, and antioxidant levels due to hypercapnia/ischemia and dissection. Changes in phosphate donors, glycosylation and amino acids reflect post-

translational and protein degradation processes that persist post-mortem. Microwave irradiation is necessary for accurately capturing in vivo metabolite concentrations in brain.

1. Introduction

Understanding the magnitude of postmortem changes in brain neurochemistry has been one of the longstanding challenges of brain metabolomic studies. Quantifying metabolites in *ex vivo* brain tissue is known to be impacted by ischemia occurring as the animal dies [103,110]. Historical methods originally used immersion of the entire animal into liquid nitrogen (-196°C) as a method of tissue fixation when studying acetylcholine concentrations in the brain [104]. However, as noted by Lust et al., it was lacking as a technique due to deep brain structures requiring sometimes as much as 75 seconds to reach 0°C, the temperature at which enzyme activity is substantially reduced [96]. This led to the creation of the freeze-blow technique [98] which very quickly removed brains from rats by insertion of two hollow probes, one which pumps pressurized air through one ear, to force the brain into another probe, inserted into the other ear, which deposits it into a chamber containing pre-cooled liquid nitrogen. This provided better results compared to whole-animal immersion in liquid nitrogen [98]. However, the primary drawback of the freeze-blowing technique is that it destroys the structural integrity of the brain, limiting its application to brain regions.

High-energy microwave irradiation was then developed to minimize the impact of post-mortem hypercapnia/ischemia on brain metabolite concentrations, as summarized in **Supplementary Table 1** [96,97,111]. Early techniques involved full-body irradiation of the animal using low intensity (1.25 kW) microwave irradiation for 6-30 seconds [111]. The full-body fixation method was shown to yield ATP, phosphocreatine and lactate comparable to whole-body immersion in liquid nitrogen [98]. Measurements of ATP with higher intensity head-focused irradiation (6 kW) for a minimum of 0.4 seconds has been observed to be comparable to freeze-blowing [97].

While studies continue to report that major brain neurotransmitters such as γ-aminobutyric acid (GABA) and glutamate remain stable without microwave irradiation [106,107], there has not been any systemic work determining whether these neurotransmitters and other metabolites within the brain are affected by hypercapnia/ischemia caused by CO_2 asphyxiation, beyond acetylcholine and those involved in energy metabolism [98,106,107]. To that end, we sought to determine 1) which brain metabolites are affected by hypercapnia/ischemia in rats; 2) whether prolonged hypercapnia/ischemia associated with a postmortem interval comparable to the typical time it takes to dissect the brains affects metabolite concentrations; and 3) whether the dissection process itself affects brain metabolite concentrations as recently reported for lipids [101]. Nuclear Magnetic Resonance (NMR) was used to measure phosphate donors / acceptors, Krebs cycle metabolites, ketones, carbohydrates (simple sugars and sugar donors), amino acids, lipids, antioxidants, neurotransmitters, nucleotides and other non-specific compounds. We hypothesized that significant changes would be observed in metabolites related to energy metabolism and in neurotransmitters, in view of prior reports demonstrating that these compounds rapidly degrade in postmortem brain tissue [96,98,107] and *ex vivo* slice preparations [112].

2. Methods

As part of another study [101], one month old Long Evans male rats obtained from Charles River (Saint-Constant, Canada) were fed the 2018 Teklad Global 18% protein rodent diet (Envigo, Madison, WI) for one month. All procedures were performed in accordance with the Canadian Council on Animal Care and were approved by the University of Toronto Animal Ethics committee.

After one month of acclimatization to the diet and vivarium, rats were randomly assigned to one of four groups. The first control group (Group 1, n=8) was subjected to high energy head-focused microwave fixation (13.5 kW for 1.6 s) followed by decapitation and brain dissection. The second group (Group 2, n=7) was euthanized by CO_2 asphyxiation for 2 minutes to induce hypercapnia/ischemia, and then subjected to head-focused microwave irradiation at 13.5 kW for 1.6 s, decapitation and brain dissection. The third group (Group 3, n=8) was euthanized by CO_2 asphyxiation for 2 minutes as Group 2, but after decapitation, the head was left intact on the bench for an average of 6.4 minutes, to mimic the dissection time for the fourth group (see next sentence), and then subjected to microwave irradiation at 13.5 kW for 1.6 s. Temperature after microwave irradiation was consistent across all animals. This group captures prolonged effects of hypercapnia/ischemia on brain metabolite concentrations. The fourth group was euthanized by CO_2, then decapitated and dissected within this time, thus examining effects of both prolonged hypercapnia/ischemia and the process of dissection, on brain metabolite levels. Variability in wait times in Group 3 was matched to dissection times in Group 4. As previously published, dissection times were 5.3±1.4 minutes for Group 1, 4.7±1.3 minutes for Group 2, 6.4 ±2.4 minutes for Group 3, and 6.6±2.5 minutes for Group 4 [101]. All excised brains were flash frozen in liquid nitrogen, were shipped to UC Davis from the University of Toronto, and stored at -80ºC until analysis at a later date. All samples were stored for approximately the same amount of time. All rats were weighed prior to euthanasia, and as previously reported, rat weights did not differ significantly between the groups [101].

The excised brains were subjected to a modified Folch extraction method using 8:4:3 chloroform:methanol:water [113] Approximately 800-1000 mg of tissue was homogenized with zircona beads in a Bullet Blender with 0.9% KCl, 1 mM ethylenediaminetetraacetic acid (EDTA)

to prepare a 50% brain homogenate by weight mixture. 600 µL of this homogenate was combined with 4.8 mL of 2:1 (v/v) chloroform:methanol containing 0.002% butylated hydroxytoluene (BHT). Samples were vortexed and centrifuged at 1000 x *g* for 10 minutes at 4 ºC. The bottom chloroform phase was removed and the samples were re-extracted with 2.8 mL of 10:1 (v/v) chloroform/methanol. The bottom chloroform phase of the second extract was removed and combined with the first extract for future lipid analysis (not part of this study). The upper aqueous phase (~2 mL) consisting of methanol:water was kept and stored at -80 ºC until NMR analysis.

Samples were thawed on ice and a 250 µL aliquot was dried with SpeedVac and reconstituted in 207 µL of deionized H_2O. 23 µL of d6-4,4-dimethyl-4-silapentane-1-sulfonic acid (DSS-d6) was added as an internal standard, and samples were adjusted to a pH of 6.85 ± 0.15 with small amounts of HCl or NaOH. Samples were stored at 4ºC until NMR spectra were acquired using a Bruker Avance 600 equipped with a SampleJet autosampler. NMR spectra were acquired with a NOESY-presaturation pulse sequence at 25 ºC as previously described [114]. The resulting spectra were phased and baseline corrected, then profiled using Chenomx NMR Suite v8.1 (Chenomx, Edmonton, Canada). A total of 60 metabolites were detected and quantified. Extraction and NMR analysis of brain samples was blinded.

2.1 Statistical Analysis

Data were analyzed using GraphPad Prism Version 9.1.0 (GraphPad Software, Inc., California, USA). Additionally, a principal component analysis (PCA) plot was generated using untransformed metabolite data to visualize differences between samples using MetaboAnalyst version 5.0. Data were first tested for normality by Shapiro-Wilk's test. Metabolites that were normally distributed were analyzed by one-way analysis of variance (ANOVA) with a post-hoc Tukey's test, while metabolites that were not normally distributed were analyzed by a Kruskal-

Wallis test with a post-hoc Dunn's test to compare between-group differences. A $P \leq 0.05$ was considered significant. There were no outlier exclusions.

3. Results

The final pH of the samples prior to NMR analysis was 6.92 ± 0.26, 6.92 ± 0.11, 6.81 ± 0.04 and 6.75 ± 0.03 in Groups 1, 2, 3 and 4, respectively. The final sample pH was not significantly different between the groups by one-way ANOVA.

Figure 1 presents a PCA plot of the unsupervised analysis. As shown, controls subjected to head-focused microwave irradiation (Group 1) were clustered separated from the CO_2-asphyxiatiated rats that were not subjected to microwave-irradiation (Group 4), with the other two groups overlapping between them. This suggests distinct metabolic profiles between the groups, particularly Groups 1 and 4.

Table 1 presents mean (SD) brain metabolite concentrations in rats 1) decapitated directly after microwave fixation (Group 1); 2) decapitated after 2 minutes of CO_2 asphyxiation followed by microwave fixation (Group 2); 3) subjected to 2 minutes of CO_2 asphyxiation, followed by decapitation and a 6.4-minute average wait prior to microwave irradiation of the head and its dissection, and 4) 2 minutes of CO_2 asphyxiation, decapitation and dissection which took an average of 6.4 minutes. As will be presented below, significant differences in many metabolites were observed in the CO_2+microwave group (Group 2), the CO_2+wait+microwave group (Group 3), and/or the CO_2 only group (Group 4) relative to the control group that received microwave fixation (Group 1) for phosphate donor, Krebs cycle, ketone, carbohydrate, amino acid, lipid,

antioxidant, neurotransmitter and nucleotide metabolism. Other non-specific metabolites were also altered.

3.1 Phosphate donor/acceptor metabolites:

Except for carnitine, all metabolites involved in brain phosphate metabolism were significantly different by one-way ANOVA or Kruskal-Wallis test. Relative to Group 1, ATP concentrations were lower in Groups 2, 3, and 4 by 4, 8 and 22-fold, respectively ($p<0.0001$). Similarly, ADP was lower in Groups 3 and 4 compared to Group 1, by 4 and 24-fold, respectively ($p<0.0001$). AMP was significantly higher in Group 2 compared to Groups 1 and 4 by 3-45 fold ($p=0.0018$). Creatine was significantly higher by 65% in Group 3 compared to Group 1, whereas phosphocreatine was significantly lower by 24- and 51-fold in Groups 3 and 4, respectively, relative to Group 1 ($p=0.0134$). GTP was lower in Groups 2, 3 and 4 by 2-5 fold compared to Group 1 ($p<0.0001$).

3.2 Krebs cycle metabolites:

Out of the Krebs cycle metabolites, acetate was significantly elevated by 3-fold in Group 4 compared to Group 1 controls ($p=0.0057$). Succinate was significantly higher in Groups 2 and 3 compared to Group 4, but none of these treatment groups differed significantly from controls (Group 1) ($p=0007$). NAD+ was detected in 4-6 out of 7-8 rats in Groups 1, 2 and 3, but was not detected in any of the rats in Group 4.

3.3 Ketone bodies:

β-hydroxybutyrate was significantly elevated by 3-fold in Group 3 compared to Group 1 ($p=0.0017$). Other ketones (acetone and acetoacetate) did not significantly differ.

3.4 Carbohydrate metabolites:

Several carbohydrate metabolites were altered by hypercapnia/ischemia. Lactate was 5-fold higher in both Groups 3 and 4 compared to Group 1 ($p=0.0007$). Conversely, glucose was significantly lower by 9-fold in Group 4 versus Group 1 ($p=0.0022$). Sugar donors, including UDP-N-Acetylglucosamine ($p=0.001$), UDP-galactose ($p=0.0457$) and UDP-glucose ($p=0011$) were significantly lower by 2-3-fold in Group 4 compared to Group 1.

3.5 Amino acids:

Of the amino acids measured, branched chain amino acids (isoleucine ($p=0.0017$), leucine ($p=0.001$), and valine ($p=0.0014$)), as well as histidine ($p=0.0341$), phenylalanine ($p=0.0027$) and tyrosine ($p=0.0056$) were significantly elevated by 2-3-fold in Group 4 compared to Group 1 controls. Glutamate was significantly lower by 28% in Group 4 compared to Group 3 (neither group differed significantly from Groups 1 and 2) ($p=0.0431$).

3.6 Lipid metabolism:

sn-Glycero-3-phosphocholine was 5-fold lower in Group 4 compared to Group 1 ($p<0.0001$). This change was paralleled by a 5-fold higher choline concentration in Group 4 compared to Group 1 ($p=001$). O-Phosphocholine and myoinositol did not differ significantly between the groups.

3.7 Antioxidants

Ascorbate (p=0.0111) and glutathione (GSH, reduced form; p=0.027) were significantly elevated in Group 2 (by 2-fold) compared to Group 1. The higher ascorbate was also significant compared to Group 4, which was comparable in concentration to Group 1.

3.8 Neurotransmitters

4-Aminobutyrate (i.e. GABA) and N-acetylaspartate, the most abundant neurotransmitters in brain, were the only two detected. 4-Aminobutyrate was approximately 2-fold higher in Groups 3 and 4 compared to Group 1 (p=0.0008). N-Acetylaspartate was 26% lower in Group 4 compared to Group 1 (p=0.0102).

3.9 Nucleotide Metabolites

Four out of 6 nucleotides changed significantly. Hypoxanthine (p=0.0025) and uracil (p=0.0014) were ~6 times higher in Group 4 compared to Group 1. Inosine monophosphate (IMP) was significantly higher by ~3-fold in Groups 2 and 3 relative to Group 1 (p=0.0004). Uridine monophosphate (UMP) 2-fold higher in Group 2 compared to Group 1 (p<0.0001).

3.10 Other Metabolites

Dimethyl sulfone was higher (2-fold) in Group 3 relative to Group 1 (p=0.0269), whereas isovalerate (p=0.0418) and methanol (p=0.0324) were significantly lower in Group 4 compared to Group 3, and did not differ from Group 1.

4. Discussion

This study demonstrated notable effects of hypercapnia/ischemia and brain dissection on multiple metabolites involved in energy pathways (phosphate donors / acceptors, Kreb's cycle and ketones), and carbohydrate, amino acid and lipid metabolism, as well as on antioxidants, neurotransmitters and nucleotides. Compared to microwave-irradiated controls, hypercapnia/ischemia and dissection depleted high energy phosphate donors such as ATP and phosphocreatine, as well as substrates that can be used for energy such as glucose, and intermediate metabolites that can act as sugar donors such as UDP-glucose and UDP-galactose. Lactate increased, reflecting a shift towards anaerobic metabolism, while amino acids (leucine, isoleucine, and valine, histidine, phenylalanine and tyrosine) increased due to ischemia/hypercapnia and dissection (Group 4) compared to microwave-irradiated controls (Group 1). GABA was higher and N-Acetylaspartate was significantly lower in Group 4 relative to Group 1, indicating a change in neurotransmitter levels due to hypercapnia/ischemia and dissection. Antioxidants (asorbate and glutathione), and several nucleotides (IMP and UMP) were higher in Groups 2 or 3 relative to Group 1, but did not differ from Group 4, suggesting that hypercapnia/ischemia increased their concentrations whereas brain dissection decreased their levels to those of the control group, likely due to degradation.

High-energy phosphate donors including phosphocreatine, ADP, ATP and GTP decreased in Groups 2, 3 and 4 compared to microwave-irradiated controls (Group 1), reflecting enhanced phosphorylation of kinases downstream of G-protein coupled receptors due to hypercapnia/ischemia. Global ischemia has been shown to activate G-protein coupled receptor signaling, consistent with our findings [115]. The reduction in brain ATP, ADP and AMP following hypercapnia/ischemia is in agreement with the findings of Veech et al and Lust et al [96,98], who found that methods that limit ischemic shock, such as freeze blowing, result in a smaller reduction

of the ratio of phosphocreatine to creatine than methods that are less effective, such as full-body liquid N_2 immersion and decapitation into liquid N_2.

Additionally, compared to microwave-irradiated controls (Group 1), lower energy metabolites such as AMP and phosphate acceptors such as creatine were higher following hypercapnia/ischemia (Groups 2 and 3). These metabolites were not significantly different in Group 4 (in which brains were dissected after CO_2 asphyxiation without microwave irradiation) compared to Group 1. This indicates that the dissection process itself further consumes phosphate groups towards kinase and G-protein receptor signaling and potentially utilizes creatine for energy, consistent with the lower values of ADP, ATP and GTP observed in Group 4 compared to Groups 2 or 3, and significantly lower values relative to Group 1. It is unlikely that the changes we observed in these phosphate donors was the result of changes in body temperature, as Nilsson demonstrated that brain tissue concentrations of these metabolites do not change as a result of lowered body temperature[116].

Hypercapnia/ischemia resulted in higher concentration of brain energy substrates including succinate (Krebs cycle metabolite), beta-hydroxybutyrate (a ketone) and lactate in Groups 2 and /or 3 compared to Group 4, as well as acetate (a gut microbiome product) in Group 4 compared to microwave-irradiated controls (Group 1). Group 4 succinate and beta-hydroxybutyrate were not different compared to control, unlike acetate and lactate which reached the highest concentration in Group 4 (versus Group 1). Because all of these metabolites can be utilized to make ATP, their increased concentrations suggest increased accumulation by the brain during hypercapnia/ischemia either due to increased synthesis in the case of succinate, beta-hydroxybutyrate [117,118] and lactate (reviewed in [119]), possibly decreased utilization due to their use in oxidative phosphorylation[120], or increased protein deacylation in the case of acetate [121], since

acetate is not known to be synthesized by the brain. One study reported the rapid acylation of acetate (to produce ATP) in cultured cells subjected to hypoxia [122], suggesting increased utilization concomitant with accumulation in rats subjected to hypercapnia/ischemia. This is not unexpected because hypercapnia followed by ischemia depletes the brain's glucose supply as evidenced by the downward trend in brain glucose concentrations in Groups 2 and 3, and the significant decrease in Group 4 relative to Group 1, making it reliant on endogenous sources such a succinate, beta-hydroxybutyrate, lactate and acetate for energy.

The decline in succinate in Group 4 relative to Group 3, and the increase in succinate in Group 3 relative to Group 4, suggests increased utilization of these energy substrates during dissection, a process which likely mimics the effects of acute traumatic brain injury induced by opening the skull, cutting through the periosteum and removing the brain [123]. Metabolic energy demands of the brain are known to increase during traumatic brain injury [124], which could explain the reduction in energy substrates (succinate and beta-hydroxybutyrate) in Group 4. This postulation is further supported by the marked reduction in phosphate donor (e.g. ATP, ADP and AMP) and glucose concentrations in Group 4 compared to the other 3 groups.

Sugar donor (UDP-N-acetylglucosamine, UCP-glucose and UDP-galactose) concentrations were significantly lower in Group 4 compared to Group 1. While UDP-glucose could be utilized as a glucose donor for energy, UDP-N-acetylglucosamine and UDP-galactose are known to be involved in post-translational modification of proteins. For instance, the transfer of N-acetylglucosamine to serine and/or threonine residues of proteins within dopaminergic neurons was shown to be necessary for the release of dopamine and the co-release of glutamic acid and GABA neurotransmitters [125], and to enhance GABAergic activity in neurons [126]. In this study, glutamate was significantly lower in Group 4 compared to Group 3, and GABA was significantly

higher in Group 3 and 4 compared to Group 1, suggesting coupling of post-translational modification processes to neurotransmitter release due to acute trauma associated with brain dissection (in Group 4).

Several amino acids (leucine, isoleucine, valine, histidine phenylalanine and tyrosine) were higher in Group 4 compared to Group 1, as were multiple nucleotides in Groups 2 (IMP and UMP), 3 (IMP) and 4 (hypoxanthine and uracil). Increased concentrations of amino acids and nucleotides is likely due to increased catabolism of proteins or RNA during hypercapnia/ischemia and dissection. Other amino acids such as phenylalanine serve as a precursor to tyrosine, which can be converted in multiple monoamine neurotransmitters including norepinephrine and dopamine [127]. Thus, the increase of both phenylalanine and tyrosine in Group 4 (versus Group 1) suggests increased turnover, potentially to compensate for the increased utilization of monoamine neurotransmitters during brain dissection [128].

Glycerophosphocholine was significantly lower, whereas choline, the main product of glycerophosphocholine breakdown higher in Group 4 compared to Group 1. Global ischemia is known to breakdown phospholipids, thus liberating phosphate to further be used for energy [129]. Our data herein, indicate that brain dissection per se rather ischemia caused the 5-fold reduction in glycerophospholipids.

The higher ascorbate and glutathione concentrations in Group 2 versus Group 1 is likely due to increased synthesis following hypercapnia/ischemia. *In vivo*, rats are known to synthesize ascorbic acid and to generate glutathione from oxidized glutathione (GSSG) [130]. Ascorbate administration has been demonstrated to protect the brain from damage secondary to hypoxic-ischemia in rats by reducing both necrosis and apoptotic cell death [131]. Similarly, glutathione has been demonstrated to prevent the decline in activity of the mitochondrial complexes in transient

ischemia [132]. Thus, endogenous synthesis/formation of these antioxidants was likely prompted by hypercapnia/ischemia. Dissection appears to have increased ascorbate utilization in Group 4, since concentrations were comparable to Group 1. One study reported increased oxidation of ascorbic acid following cortical ablation [133], a scenario which could induce trauma similar to brain dissection.

While concentrations of ATP and ADP in microwave-irradiated rats were significantly lower by 33% and 61% respectively than previously reported, we found that lactate, the major marker for ischemia, as well as phosphocreatine, were similar in concentrations to the literature; **Supplementary Table 1** [96,97]. This is possibly due to the difference in measurement methods, as both Medina et al. and Lust et al. used a Lowry assay [134] rather than NMR spectrometry to quantify the concentrations of these metabolites, or possibly due to differences in microwave output, as Medina and Lust used 6 kW while we used 13.5 kW. The higher energy output would result in the faster fixation of tissue, resulting in concentrations that more closely match those *in vivo*.

In summary, this study found that compared to head-focused microwave irradiation, both CO_2-induced hypercapnia/ischemia and brain dissection altered the concentration of metabolites involved in energy pathways, glycosylation, proteolysis, neurotransmission, nucleotide synthesis, lipid signaling and antioxidant capacity. Our findings 1) provide new information on the physiological effects of hypercapnia/ischemia and dissection on the brain metabolome, and 2) suggest that in studies which examine metabolomics in brain tissue, ischemia/hypercapnia and dissection may mask subtle differences in metabolites that could be captured by using microwave fixation.

Conflicts of Interest: None to declare

Author contributions: D.A.S. and A.Y.T. conceived the study. D.A.S. prepared sample extracts for NMR, analyzed acquired spectra, and prepared the manuscript. Y.O. prepared sample extracts from tissue samples. A.H.M. and R.P.B. performed the work with the animals and obtained tissue samples. C.M.S. assisted in obtaining NMR spectra. A.Y.T. provided guidance in data analysis and manuscript preparation. All authors reviewed the manuscript.

Funding: This research was supported by the Hellman Family Foundation (A.Y.T.).

Figure Legends:

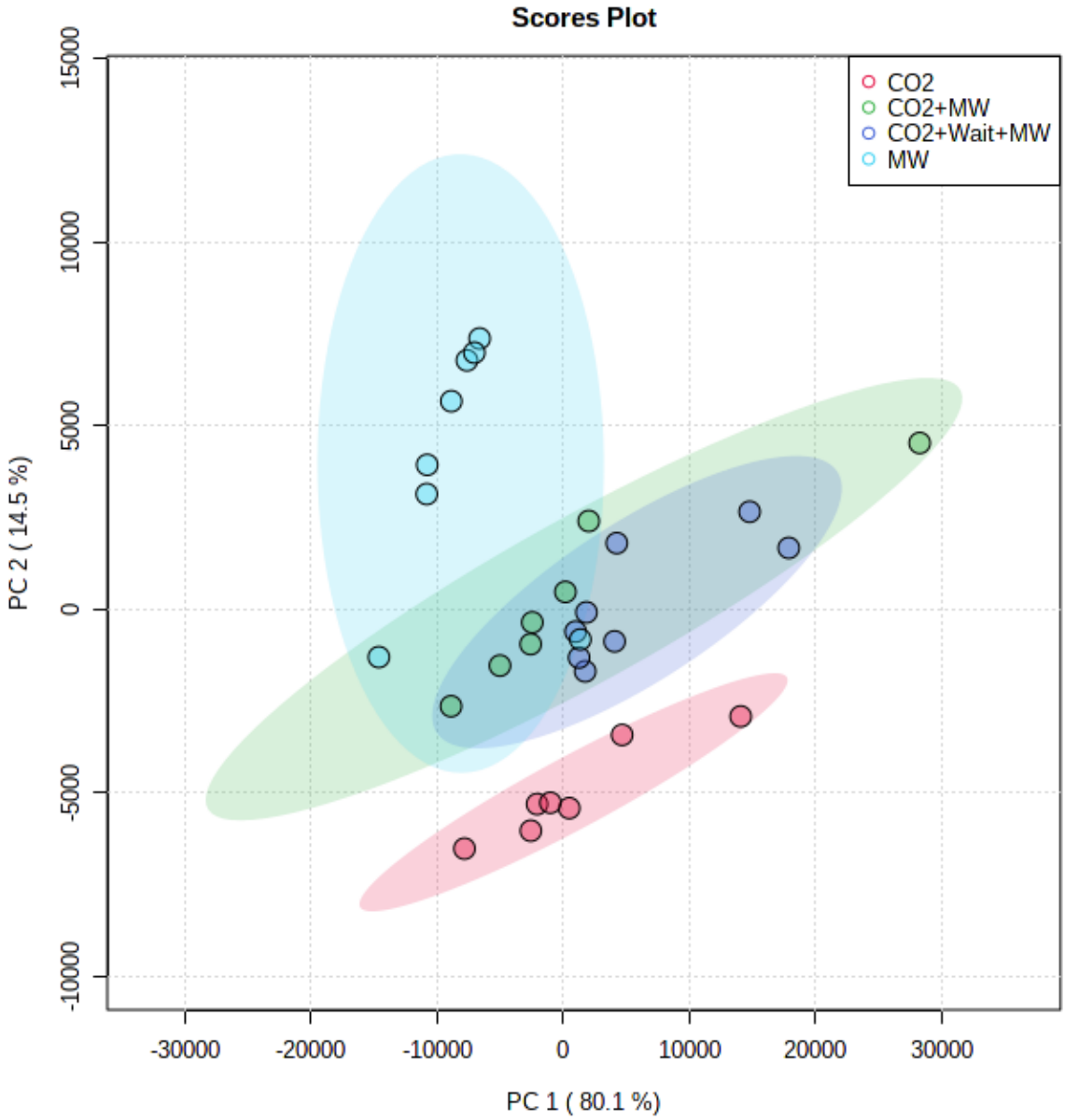

Figure 1: PCA plot of brain metabolites.

Table 1: Concentrations of identified metabolites in rat brains subjected to differing methods of fixation. All concentrations are expressed in units of nmol/g and data are presented as mean±SD. Provided p-values indicate the significance of a one-way ANOVA test with post-hoc Tukey test if normally distributed, or a Kruskal-Wallis test with post-hoc Dunn's test if not normally distributed Superscript letters indicate group similarity as determined by post-hoc test. For metabolites that were not detected in every sample within a group, the number of samples in which the metabolite was detected is in superscript. Metabolites are grouped by general function.

Phosphate Donors	Group 1 (MW)	Group 2 (CO_2+MW)	Group 3 (CO_2+Wait+MW)	Group 4 (CO_2)	*p*
ATP	1039.5±626.8^{a}	296.2±134.7^{b}	123.1±53.6^{b}	46.5±25.1^{b}	<0.0001
ADP	512.2±241.4^{a}	489.5±275.9^{ab}	136.4±55.6^{cd}	21.5±12.5^{d}	<0.0001
AMP	282.2±197.1^{a}	944.2±603.5^{b}	548.2±514.0^{ab}	21.1±9.9^{a}	0.0018
Creatine	7192.9±2074.1^{a}	10624.8±4964.5^{ab}	11856.1±2697.7^{b}	8635.0±2709.7^{a} ^{b}	0.0134
Creatine phosphate	2604.0±1085.6^{a}	128.4±112.8^{ab}	108.7±60.4^{b}	50.9±30.1^{b}	0.0003
GTP	298.7±118.8^{a}	165.2±49.0^{b}	118.6±38.8^{bc}	56.9±26.0^{c}	<0.0001
Krebs Cycle and Oxidative Metabolism					
Succinate	134.6±246.9^{ab}	420.4±208.9^{b}	626.8±382.8^{b}	18.8±19.8^{a}	0.0007
Fumarate	96.3±42.6	125.5±144.7	200.4±211.3	196.9±94.7	0.1785
Acetate	782.6±303.7^{a}	1414.1±2059.4^{a}	1491.3±1125.6^{ab}	2206.9±562.4^{b}	0.0057
Carnitine	83.8±37.5	99.5±72.5	87.2±33.0	81.4±30.9	0.9878
NAD+	219.6±36.7$^{6 \text{ out of } 8}$	267.7±51.9$^{5 \text{ out of } 7}$	139.1±80.5$^{4 \text{ out of } 8}$	ND$^{0 \text{ out of } 7}$	
NADH	ND	ND	ND	ND	
Ketone Bodies					
Acetoacetate	15.5±7.3	28.4±15.4	26.7±12.6	21.1±11.1	0.1588
Acetone	24.5±7.8	32.3±17.8	31.5±6.6	24.1±6.5	0.1007
β-Hydroxybutyrate	12.3±9.1^{a}	20.2±10.8^{ab}	39.3±13.3^{b}	23.9±7.2^{ab}	0.0017
Carbohydrate Metabolites					

Lactate	2955.5±4077.1[a]	12413.1±8170.4[ab]	15976.6±4542.8[b]	14229.5±4902.0[b]	0.0007
Glucose	881.6±568.9[a]	255.4±224.0[ab]	180.8±105.7[ab]	101.0±51.7[b]	0.0022
Glucose-1-phosphate	ND	ND	ND	ND	
Glucose-6-phosphate	384.8±234.7	270.0±179.3	181.4±129.2	136.2±61.9	0.1567
UDP-N-Acetylglucosamine	79.3±20.0[a]	72.0±12.6[a]	66.9±16.2[a]	35.5±25.4[b]	0.001
UDP-galactose	89.4±43.1[a]	61.8±20.4[ab]	69.2±41.3[ab]	36.2±22.3[b]	0.0457
UDP-glucose	83.6±24.1[a]	79.5±21.2[a]	75.4±46.3[a]	33.0±12.4[b]	0.011
Amino Acids					
Alanine	578.7±249.9	797.2±676.4	1074.3±431.7	1021.9±337.2	0.0194
Aspartate	2693.7±771.8	3903.2±3426.5	3768.6±1369.9	4210.3±1250.3	0.0835
Glutamate	10842.9±2383.7[ab]	11680.8±5242.4[ab]	13020.7±2963.6[a]	7834.4±2495.9[b]	0.0431
Glutamine	5106.8±899.8	4634.7±993.6	5503.1±601.2	4572.9±1645.9	0.1538
Glycine	1226.2±532.2	1494.4±1439.6	1799.9±919.6	1981.5±585.1	0.0653
Histidine	59.2±22.6[a]	100.7±64.1[ab]	96.1±29.2[ab]	112.4±44.0[b]	0.0341
Isoleucine	42.2±24.1[a]	66.2±84.7[a]	90.0±47.6[ab]	140.6±42.2[b]	0.0017
Leucine	91.7±38.8[a]	145.6±165.9[a]	174.8±76.6[ab]	304.0±70.7[b]	0.001
Lysine	308.7±130.6	388.2±241.2	334.6±89.9	483.7±100.9	0.0574
Phenylalanine	64.0±21.5[a]	82.1±72.3[a]	92.2±33.0[ab]	177.2±55.1[b]	0.0027
Threonine	666.5±196.8	882.6±625.8	958.7±292.7	744.9±270.4	0.1995
Tryptophan	ND	ND	ND	ND	
Tyrosine	93.1±41.2[a]	112.9±85.0[a]	138.6±43.0[ab]	200.4±46.3[b]	0.0056
Valine	92.1±34.3[a]	130.6±128.9[a]	160.3±58.5[ab]	207.2±49.5[b]	0.0014
Lipid Signaling					
Choline	145.3±119.7[a]	144.6±223.1[a]	191.7±77.4[ab]	667.7±202.4[b]	0.001
O-Phosphocholine	561.2±152.4	683.3±547.7	796.3±350.9	619.8±284.5	0.498

sn-Glycero-3-phosphocholine	637.1±130.3[a]	809.8±190.4[a]	822.6±133.6[a]	137.3±61.8[b]	<0.0001
myo-Inositol	6658.3±1465.4	7346.0±3019.7	8083.1±1708.9	6226.5±1885.4	0.3401
Antioxidants					
Ascorbate	73.3±63.3[a]	146.1±51.4[b]	77.2±38.8[ab]	58.5±22.4[a]	0.0111
Carnosine	52.6±30.3	62.7±51.2	81.5±36.7	94.1±37.1	0.1093
Glutathione-SH	77.2±15.4[a]	134.8±56.3[b]	103.0±20.2[ab]	132.5±53.4[ab]	0.027
Neurotransmitters					
4-Aminobutyrate	1688.4±437.6[a]	2438.1±1759.6[ab]	3132.6±1118.6[b]	3519.6±1129.6[b]	0.0008
N-Acetylaspartate	7316.9±1469.4[ab]	7829.5±2227.9[ab]	8598.8±1330.6[a]	5416.0±1749.9[b]	0.0102
Nucleotide Metabolites					
Adenosine	25.6±27.3	27.4±20.1	22.4±6.7	19.1±8.3	0.6229
Hypoxanthine	108.9±114.3[a]	257.3±442.4[a]	416.8±299.9[ab]	640.8±186.2[b]	0.0025
IMP	38.1±26.8[a]	98.0±45.3[b]	96.4±41.5[b]	28.7±18.4[a]	0.0004
Inosine	823.8±851.5	763.5±862.4	1663.0±442.8	1360.1±451.8	0.0791
UMP	34.5±21.3[ac]	80.0±25.4[b]	49.6±24.1[a]	17.5±5.1[c]	<0.0001
Uracil	20.7±6.8[a]	79.1±129.5[ab]	74.8±75.4[ab]	114.8±40.9[b]	0.0014
Other Metabolites					
3-Hydroxyisovalerate	2.6±1.0	3.4±2.3	3.6±1.5	3.8±1.5	0.2171
Benzoate	15.5±5.0	21.3±18.2	16.0±5.6	21.2±12.4	0.7807
Dimethyl sulfone	17.9±5.4[a]	26.5±14.5[ab]	32.6±9.8[b]	24.7±10.5[ab]	0.0269
Ethanol	17.9±14.3	25.0±19.1	27.0±17.0	23.0±12.0	0.4776
Formate	533.3±76.3	604.0±225.6	678.7±168.4	477.3±127.0	0.0515
Isovalerate	11.2±2.7[ab]	13.3±8.2[ab]	13.5±2.9[a]	10.7±4.9[b]	0.0418
Methanol	771.8±185.4[ab]	884.2±409.3[ab]	1014.5±275.9[a]	666.4±134.0[b]	0.0324
Nicotinurate	97.9±51.9[5 of 8]	122.5±117.8[5 of 7]	179.8±69.7[7 of 8]	157.6±41.1[8 of 8]	0.2543
Pantothenate	22.8±6.5	24.1±8.6	31.8±8.6	22.7±8.0	0.1286

Propylene glycol	20.8±3.6	22.6±8.0	30.0±14.8	22.4±5.0	0.4075
Quinolinate	ND	ND	ND	ND	
Sarcosine	12.6±3.1	12.7±7.0	14.6±5.1	9.8±6.6	0.1632
Taurine	4735.0±904.9	5126.9±1892.8	5837.0±975.6	4176.4±1352.7	0.0632
Urea	2625.7±1065.4	2828.0±933.0	2734.2±691.9	2256.3±841.4	0.6486

Supplementary Table 1: Metabolite concentrations reported by other authors. Concentrations are expressed as mean±SD in units of μmol/g wet brain. Freeze-blowing follows the protocol of Veech et al [98]. Cells marked with ND denote that the metabolite was not measured.

	Lust 1973 [96]	Veech 1973 [98]	Balcom 1976 [106]	Medina 1975 [97]	Balcom 1975 [107]	Nihei 1989 [108]
Phosphate Donors						
ATP	2.41±0.08 Freeze-blown, 1.68±0.03 MW, 1.79±0.06 Decapitation into liquid N_2	2.45±0.05 Freeze-blown, 1.69±0.02 MW, 1.54±0.15 Decapitation into Liquid N_2	ND	2.372±0.102 MW, 2.51±0.06 Freeze-blown	ND	ND
ADP	ND	0.561±0.022 Freeze-blown, 1.32±0.02 MW, 0.657±0.037 Decapitation into liquid N_2	ND	0.646±0.015 MW, ND Freeze-blown	ND	ND
AMP	ND	0.041±0.001 Freeze-blown, 0.399±0.011 MW, 0.403±0.039 Decapitation into liquid N2	ND	0.060±0.004 MW, ND Freeze-blown	ND	ND
Creatine	ND	5.12±0.05 MW, ND MW, 7.48±0.33 Decapitation into liquid N_2	ND	ND	ND	ND
Creatine phosphate	4.00±0.10 Freeze-blown, 1.72±0.08 MW, 1.41±0.03 Decapitation into liquid N_2	4.05±0.07 Freeze-blown, 1.68±0.08 MW, 1.29±0.13 Decapitation into Liquid N_2	ND	3.715±0.056 MW, 3.55±0.11 Freeze-blown	ND	ND
GTP	ND	ND	ND	ND	ND	ND

Krebs Cycle and Oxidative Phosphorylation						
Succinate	ND	ND	ND	ND	ND	ND
Fumarate	ND	ND	ND	ND	ND	ND
Acetate	ND	ND	ND	ND	ND	ND
Carnitine	ND	ND	ND	ND	ND	ND
NAD+	ND	ND	ND	ND	ND	ND
NADH	ND	ND	ND	ND	ND	ND
Ketone Bodies						
Acetoacetate	ND	ND	ND	ND	ND	ND
Acetone	ND	ND	ND	ND	ND	ND
β-Hydroxybutyrate	ND	ND	ND	ND	ND	ND
Carbohydrate Metabolites						
Lactate	1.23±0.07 Freeze-blown, 1.71±0.15 MW, 3.16±0.13 Decapitation into liquid N_2	1.23±0.07 Freeze-blown, 1.71±0.15 MW, 3.16±0.13 Decapitation into liquid N2	ND	1.244±0.37 MW, 1.39±0.09 Freeze-blown	ND	ND
Glucose	ND	0.962±0.084 Freeze-blown, ND MW, 0.199±0.029 Decapitation into liquid N2	ND	1.185±0.114 MW, 1.37±0.05 Freeze-blown	ND	ND
Glucose-1-Phosphate	ND	ND	ND	ND	ND	ND
Glucose-6-Phosphate	ND	0.162±0.001 Freeze-blown, MW, 0.040±0.008 Decapitation into liquid N2	ND	ND	ND	ND
UDP-N-Acetylglucosamine	ND	ND	ND	ND	ND	ND
UDP-Galactose	ND	ND	ND	ND	ND	ND
UDP-Glucose	ND	ND	ND	ND	ND	ND
Amino Acids						
Alanine	ND	ND	ND	ND	ND	ND

Aspartate	ND	2.46±0.06 Freeze-Blown, 1.32±0.02 MW, 0.657±0.037 Decapitation into liquid N2	ND	ND	ND	ND
Glutamate	ND	11.20±0.25 Freeze-Blown, ND MW, 9.92±0.64 Decapitation into liquid N2	11.16±0.27 MW (zero time), 11.10±0.31 MW (after 30 minutes), 11.23±0.40 decapitation at RT (zero time), 10.44±0.48 (after 30 minutes)	ND	ND	ND
Glutamine	ND	ND	ND	ND	ND	ND
Glycine	ND	ND	ND	ND	ND	ND
Histidine	ND	ND	ND	ND	ND	ND
Isoleucine	ND	ND	ND	ND	ND	ND
Leucine	ND	ND	ND	ND	ND	ND
Lysine	ND	ND	ND	ND	ND	ND
Phenylalanine	ND	ND	ND	ND	ND	ND
Threonine	ND	ND	ND	ND	ND	ND
Tryptophan	ND	ND	ND	ND	ND	ND
Tyrosine	ND	ND	ND	ND	ND	ND
Valine	ND	ND	ND	ND	ND	ND
Lipid Signaling						
Choline	ND	ND	ND	ND	ND	ND
O-Phosphocholine	ND	ND	ND	ND	ND	ND
sn-Glycero-3-phosphocholine	ND	ND	ND	ND	ND	ND
myo-Inositol	ND	ND	ND	ND	ND	ND
Antioxidants						
Ascorbate	ND	ND	ND	ND	ND	ND
Carnosine	ND	ND	ND	ND	ND	ND
Glutathione	ND	ND	ND	ND	ND	ND
Neurotransmitters						
4-Aminobutyrate	ND	ND	ND	ND	1.82±0.6 MW (zero time), 1.84±0.08	ND

					MW (after 30 minutes), 2.14±0.06 decapitation at RT (zero time), 2.69±0.20 (after 30 minutes)	
N-Acetylaspartate	ND	ND	ND	ND	ND	ND
Nucleotide Metabolites						
Adenosine	ND	ND	ND	ND	ND	ND
Hypoxanthine	ND	ND	ND	ND	ND	0.786±0.013 after 1 hour, then MW, 0.034±0.003 MW immediately
IMP	ND	ND	ND	ND	ND	ND
Inosine	ND	ND	ND	ND	ND	ND
UMP	ND	ND	ND	ND	ND	ND
Uracil	ND	ND	ND	ND	ND	ND
Miscellaneous						
3-Hydroxyisovalerate	ND	ND	ND	ND	ND	ND
Benzoate	ND	ND	ND	ND	ND	ND
Dimethyl sulfone	ND	ND	ND	ND	ND	ND
Ethanol	ND	ND	ND	ND	ND	ND
Formate	ND	ND	ND	ND	ND	ND
Isovalerate	ND	ND	ND	ND	ND	ND
Methanol	ND	ND	ND	ND	ND	ND
Nicotinurate	ND	ND	ND	ND	ND	ND
Pantothenate	ND	ND	ND	ND	ND	ND
Propylene glycol	ND	ND	ND	ND	ND	ND
Quinolinate	ND	ND	ND	ND	ND	ND
Sarcosine	ND	ND	ND	ND	ND	ND
Taurine	ND	ND	ND	ND	ND	ND
Urea	ND	ND	ND	ND	ND	ND

Antioxidant, Transmethylation, and Energy pathways are altered in Postmortem Pre-frontal Cortex of Alzheimer's Disease Patients Without Vascular Disease

Duncan A. Sylvestre[1,2], Danielle J. Harvey[3], Yurika Otoki[1,4], Brittany N. Dugger[5], Lee-Way Jin[5], Carolyn M. Slupsky[1,2] and Ameer Y. Taha[1,*]

[1] Department of Food Science and Technology, University of California, Davis
[2] Department of Nutrition, University of California, Davis
[3] Department of Public Health Sciences, University of California, Davis
[4] Food and Biodynamic Laboratory, Graduate School of Agricultural Science, Tohoku University, Sendai, Miyagi, Japan.
[5] Department of Pathology and Laboratory Medicine, University of California, Davis

*To whom correspondence should be addressed.
Ameer Y. Taha
Department of Food Science and Technology, College of Agriculture and Environmental Sciences, University of California Davis, One Shields Avenue, Davis, CA, USA 95616
Phone: (+1) 530-752-7096; Email: ataha@ucdavis.edu

Keywords: Metabolomics, Biomarkers, Alzheimer's Disease, Neurotransmitters, Vascular Disease

Running Title: Antioxidant, Transmethylation, and Energy pathways are altered in Postmortem Pre-frontal Cortex of Alzheimer's Disease Patients Independent of Vascular Disease

Abbreviations List

- Aβ: Amyloid-beta
- AD: Alzheimer's Disease
- BHT: Butylated hydroxytoluene
- NMR: Nuclear Magnetic Resonance
- CeVD: Cerebrovascular Disease
- DSS-d6: d6-4,4-Dimethyl-4-silapentane-1-sulfonic acid
- EDTA: Ethylene diaminetetraacetic acid
- iNOS: Inducible Nitric Oxide Synthase
- ITG: Inferior Temporal Gyrus
- MFG: Middle Frontal Gyrus
- NFT: Neurofibrillary Tangle
- PET: Positron Emission Tomography
- PMI: Postmortem Interval

Abstract

Understanding brain metabolic changes that differentiate Alzheimer's Disease (AD) from underlying cerebrovascular disease (CeVD) pathology remains an unresolved topic. This study sought to measure energy, neurotransmitter, lipid, carbohydrate, amino acid and antioxidant pathways affected by AD and CeVD using Nuclear Magnetic Resonance. Metabolites were measured in postmortem pre-frontal cortex of non-demented controls and AD patients with and without CeVD. Linear regression analysis was used to test for AD and CeVD interactions, while adjusting for postmortem interval and age. Fumarate, glutathione, and sarcosine were decreased in AD patients without CeVD, compared to controls without CeVD. 2-hydroxybutyrate was negatively associated with age and postmortem interval in AD patients without CeVD. This study demonstrates reductions in transmethylation (sarcosine), antioxidant capacity (glutathione and 2-hydroxybutyrate), and energy metabolism (fumarate) in AD, changes which were no longer apparent in individuals with concurrent CeVD. The findings reflect AD-specific metabolomics changes that could distinguish AD from AD with CeVD.

Introduction

Alzheimer's Disease (AD), the most common form of dementia, is characterized by gradually worsening memory and executive function[1]. AD accounts for 50-70% of all dementia cases[135]. While it is associated with the buildup of amyloid-beta (A_β) plaques and neurofibrillary tangles (NFTs)[1], efforts to target A_β and NFTs therapeutically have not been successful and to date there is no effective treatment[136].

AD is complicated by the presence of several co-pathologies of which cerebrovascular disease (CeVD) is the most common[8], co-occurring in 64%-80% of AD cases[10,72]. CeVD is associated with the presence of diffuse white matter hyperintensities on MRI, which have been attributed to reduced blood flow within the brain[137,138], resulting in significant ischemia and impairment in executive function, attention, and memory[81]. CeVD is diagnosed based on either a composite lesion score that evaluates the presence of large infarcts, lacunes, and leucoencephalopathy[88], an evaluation of one of six subtypes of CeVD associated with either infarcts, cerebral hypoperfusion, or vascular changes associated with AD pathology[87], or a staging system that evaluates the severity of vascular changes beginning with modifications to vessel walls and culminating in large cortical infarcts[86]. Even in cases without evidence of mixed dementia, as many as 80% of patients diagnosed with AD also present vascular pathology including lacunes, infarcts, cerebral microbleeds, arteriosclerosis, and cerebral amyloid angiopathy, suggesting it may be an important contributor to AD pathogenesis and prognosis[139].

While it is possible to image A_β protofibrils and misfolded tau using Positron Emitting Tomography (PET)[140], metabolomics can help to understand metabolic changes concurrent with disease pathology. In the neocortex of AD patients, taurine and alanine were shown to increase compared to neocortex of healthy age matched controls[141]. Another study noted decreases in N-

acetylaspartate and *myo*-inositol in the superior temporal cortex of AD patients relative to controls[142], and another study observed decreased concentrations of GABA, N-acetylaspartate, and choline in the inferior temporal gyrus in AD patients relative to controls[95]. These changes were inversely correlated with Braak NFT stage and CERAD scores[95]. To our knowledge, all metabolomic studies performed in postmortem AD brains have not tested for the confounding effects of CeVD.

Individuals with the APOE4/4 genotype are known to present with increased incidence and earlier onset of AD compared to individuals with the more common APOE3/3 genotype[143], and the APOE4 gene has been associated with increased arginine uptake[144]. Arginine serves as an important modulator of macrophages and microglia through the inducible Nitric Oxide synthase (iNOS) pathway[145], thereby implicating this pathway in AD. It is not known whether arginine metabolism is affected by CeVD.

Brain metabolomic changes have also been observed in animal models of AD. Astrocytic synthesis of glycolytic L-serine was shown to be reduced in a mouse model of AD[146], where it acts as a precursor to a co-agonist of NMDA receptors required for synaptic plasticity. Intracellular lactate production was higher in the same mouse model, likely due to a deficit in glucose availability or utilization[146]. Further, a 21% increase in the parahippocampal concentration of L-arginine in 13 month old APPswe/PS1ΔE9 mouse model along with simultaneous increases in concentrations of its downstream metabolites L-ornithine and L-citrulline have been observed[147]. Bergin *et al.* also noted that glutamate and GABA did not change between wild type and transgenic mice[147].

The role of bioactive metabolites and their related pathways has not been studied in AD patients with CeVD. Because CeVD pathology is different from AD, it can either present a

unique metabolomics signature or mask changes in metabolite levels associated with AD. However, there may also be commonalities that are present due to the same mechanisms responding to AD-related insults and CeVD related insults, such as gliosis and other inflammatory processes, which are not useful for discriminating between disease states. In the present study, we used nuclear magnetic resonance (NMR) metabolomics to probe for disease-specific metabolomic signatures in postmortem pre-frontal cortex of AD and non-demented controls with or without CeVD. Prefrontal cortex was chosen due to the presence of plaques and NFTs in the advanced phases of the disease[6].We hypothesized that CeVD and AD would have unique metabolomic signatures that could be used to differentiate the two.

Methods

This study assessed a total of 41 samples collected from the University of California Davis Alzheimer's Disease Center (UCD-ADC) brain bank. The details of cases utilized in this study are described in a prior publication (Otoki et al)[148] and summarized in **Supplementary Table 1**. Descriptive statistics (age, sex, PMI, and Braak stage) are summarized in **Table 1.** Samples were chosen based on pathological criteria according to the NIA-Alzheimer's association guidelines[15,149]; six such cases received a diagnosis of CeVD. Controls (N=20) were defined as cases with no likelihood of AD according to the NIA-Alzheimer's association guidelines. Seven patients in the AD group presented cases consistent with Lewy body Disease, and one with corticobasal degeneration. Within the control group, one case had a diagnosis of progressive supranuclear palsy, one had a diagnosis of Lewy body disease, and one had a diagnosis of frontotemporal dementia. Four control patients were diagnosed with CeVD. Patients with CeVD are marked as such in **Supplementary Table 1**.

Between 50-200mg of pre-frontal cortex containing both grey and white matter was transferred to 2mL microcentrifuge tubes pre-cooled on dry ice. Polar metabolites were separated from lipids using a modified "Folch" extraction mixture containing 8:4:3 chloroform:methanol:aqueous solution . To each sample, an aqueous solution of 1 mM ethylenediaminetetraacetic acid (EDTA) and 0.9% KCl (w/v) was added to reach a final volume of 1200µL. Samples were then homogenized with zirconia beads in a Bullet Blender Storm 24 (Next Advance, Averill Park, NY, USA) for 30 seconds, three to five times. Between homogenization runs, samples were cooled in a -20°C freezer for approximately 2 to 4 minutes. The resulting homogenate was mixed with additional aqueous solution to bring to total volume, including tissue, to a final volume of 1500 µL. Six mL of pre-cooled 2:1 chloroform:methanol containing 0.002% butylated hydroxytoluene (BHT) was added to the homogenate. This extract was centrifuged at 1000g for 10 minutes at 0°C in a Solvall RT 6000 (Bio Surplus, San Diego, CA, USA) to separate the organic chloroform layer from the upper methanol-water aqueous phase. The lower chloroform layer was removed, and the remaining aqueous phase was re-extracted with an additional 3.5mL of 10:1 chloroform:methanol and centrifuged again at 1000g for 10 minutes at 0°C. The lower chloroform phase was removed, and the upper aqueous layer was decanted and stored at -80°C until NMR analysis.

A total of 2mL of aqueous extract was recovered, all of which was dried via SpeedVac and reconstituted in 207µL of DI H_2O. 23µL of d6-4,4-Dimethyl-4-silapentane-1-sulfonic acid (DSS-d6) was added as an internal standard, and samples were pH adjusted with small amounts of HCl and NaOH to bring the pH within a range of 6.85±0.15. Samples were then stored at 4°C until NMR spectra were acquired using a Bruker Avance 600 equipped with a SampleJet

autosampler. NMR spectra were acquired with a NOESY presaturation pulse as described previously[114]. The spectra were then phase and baseline corrected, and profiled using Chenomx NMR Suite v.8.1 (Chenomx, Edmonton, Canada). A total of 52 metabolites were detected and quantified. Extraction and NMR analysis of tissue samples was blinded.

Statistical Analysis

Patients with age >90 years were treated as having an age of 90 to comply with HIPAA regulations. Age, postmortem interval (PMI), Sex, and Braak NFT stage were compared for patients groups of: Control (lacking a clinicopathologic diagnosis of AD), AD, Control+CeVD and AD+CeVD groups with a one-way ANOVA with post-hoc Tukey test. Metabolite data were $\log_{10}$-transformed in Excel, and PMI and age were centered on the overall mean. The data were subjected to multi-linear regression analysis in GraphPad Prism Version 9.1.0 (GraphPad Software, Inc., California, USA) incorporating AD versus control and CeVD versus non-CeVD as categorical variables and mean-centered PMI and age as continuous variables. ApoE genotype was not included in the regression to minimize the risk of co-linearity, since the majority of the AD subjects (75%) had one or two alleles of the apoE4[148]. In contrast, only 11% of controls had one or two apoE4 alleles[148]. We tested for main effects of each variable, and AD/control interactions with each variable. A $P \leq 0.05$ was considered significant. There were no outlier exclusions.

Results

Table 1 presents descriptive statistics for patients. As shown, there is no difference in sex between groups, nor is there a difference in age or PMI by one-way ANOVA. Braak NFT stage differed based on AD status, with no differences between the AD+CeVD and AD groups, as well as the Control+CeVD and control groups.

Out of a total of 52 metabolites detected and quantified by NMR, four were significant by the multi-linear regression model. **Table 2** presents descriptive data (mean±SD) for log-transformed brain metabolite concentrations that were significantly different between controls and AD patients with and without CeVD. None of these metabolites were significant by one-way ANOVA. All metabolites measured, including those not significant in the multiple regression model, are presented in **Supplementary Table 2**.

Table 3 presents the results of the multiple linear regression model. As shown, main effects or interactions were observed for sarcosine, glutathione, fumarate and 2-hydroxybutyrate. There was a main effect of AD without CeVD on sarcosine, glutathione, and fumarate concentrations, which were significantly lower in AD without CeVD relative to controls without CeVD. These differences were not significant in subjects with AD and CeVD compared to controls with CeVD. Additionally, for sarcosine, there was a main effect of PMI, and for glutathione, there was a main effect of age and AD x PMI interaction, suggesting that differences between AD and controls (both without CeVD) for these metabolites occurred at the centered mean PMI or age. 2-hydroxybutyrate was negatively correlated with PMI and age in the AD group without CeVD.

Discussion

This study found differences in metabolites associated with antioxidant synthesis (glutathione and 2-hydroxybutyrate), transmethylation (sarcosine), and cellular respiration (fumarate), in AD subjects without CeVD when accounting for age and PMI. Compared to controls without CeVD pathology, fumarate, glutathione, and sarcosine were reduced in AD

subjects without CeVD. 2-Hydroxybutyrate was negatively associated with PMI and age in the AD group without CeVD.

Consistent with the changes in 2-hydroxybutyrate (lower in older AD patients without CeVD), prior studies have observed reduced *in vivo* concentrations of glutathione in the prefrontal cortex and parietal cortex of AD patients compared to pathologically normal controls[150,151]. 2-Hydroxybutyrate is a byproduct of an intermediate step of glutathione synthesis, which means that changes in its concentration likely reflect changes in the turnover of glutathione. One possible reason for the reduction of 2-hydroxybutyrate or glutathione (based on prior studies) could be due to interactions of antioxidant pathways with soluble oligomeric Aβ, which has been observed to cause changes in the redox state, and decrease intracellular glutathione concentrations in human neuronal cell culture[152]. This change in antioxidant metabolism could also explain the effect of age and PMI on 2-hydroxybutyrate in the AD group; both likely reduce antioxidant tissue status.

Notably, other studies have shown glutathione to increase in the inferior temporal gyrus and the middle frontal gyrus of AD subjects[95]. The inferior temporal gyrus and middle frontal gyrus are the first to be affected by AD pathology, while the prefrontal cortex is largely spared until late in disease progression[6], suggesting potential adaptive mechanisms for glutathione turnover depending on the disease stage. Alternatively, increased glutathione concentrations in the inferior temporal gyrus and the middle frontal gyrus and reductions in cortical areas of AD patients may reflect region-specific adaptive changes to oxidative stress, which has been observed to increase in AD[153].

Sarcosine was decreased in AD patients without CeVD compared to controls without CeVD. Sarcosine is involved in transmethylation pathways. It can be formed either as a methyl

acceptor by glycine-*N*-methyltransferase[154], which acts on S-adenosylmethionine, or through conversion of betaine to dimethylglycine by betaine homocysteine methyltransferase[155] and subsequent oxidation of dimethylglycine to sarcosine. These changes could be the result of altered flux in the transmethylation pathways, and changes in transmethylation metabolites S-adenosylhomocysteine and S-adenosylmethionine have been observed to decrease in the ITG and MFG of AD patients, and to correlate with disease severity[95]. Additionally, serine homocysteine, a precursor to S-adenosylmethionine was shown to increase in both AD and vascular dementia compared to controls[156].

Fumarate is a Krebs cycle intermediate. The observed decrease in fumarate concentration in AD patients without CeVD compared to controls without CeVD could be indicative of an energy deficit due to reduced flux through the Krebs cycle. Reductions in glucose uptake in the brain have been demonstrated in AD[27], as have reductions in ATP synthesis in neuronal AD cell models[157]. Further, in mouse models of AD, a mitochondrial bioenergetic deficit potentially caused by reduced glycolysis and Krebs cycle flux, was found to directly increase Aβ plaque deposition in the brain[158]. Another contributing factor to this could be changes in cell populations, possibly through increased microglial apoptosis[159].

One hypothesis of why we did not observe metabolomic changes that others such as Mahajan *et al.* [95] noted was because we took the PMI into account. Mahajan *et al*. did not include the PMI in their statistical model and instead matched AD and control case postmortem intervals. In the present study, we included PMI as a potential confounder in our multiple linear regression model. As indicated by the regression analysis, PMI affected concentrations of sarcosine and 2-hydroxybutyrate.

The differences between brain metabolite levels in AD versus controls were diminished when CeVD was included in the regression analysis. Our findings emphasize the need to account for the heterogeneous presentations of AD in postmortem brain metabolomic studies as well as heterogeneity within CeVD such as temporal aspects, locations, and types of pathologies. This should be further investigated in a larger cohort, as only a few subjects (4 controls and 6 AD) had concurrent CeVD during postmortem pathological examination.

PMI was shown to affect the concentration of some metabolites (2-hydroxybuturate, sarcosine). In a prior rat study (unpublished), we found post-mortem ischemia altered many brain metabolites, including glutamate, ATP, ADP, phosphocreatine, lactate, glucose, and glutathione. It is not known how prolonged postmortem ischemia, as is the case in humans, alters these compounds. Additionally, we did not account for potential differences in agonal states prior to death for the patients, which may alter brain metabolite levels. *In vivo* evaluation of metabolite concentrations (e.g. with PET) might better inform on brain metabolite changes compared to postmortem metabolomics, as many metabolite changes may have been masked by the effects of postmortem ischemia and agonal states.

There are several limitations of this study. First, our sample contained a mixture of grey and white matter. While this provides a representative picture of changes across the brain as a whole, this study could not evaluate changes specific to either grey or white matter. We also did not control for sex in our statistical model as a result of our limited cohort, but this was also done as there was not a significant difference in sex between the groups. We also did not have an equal distribution of ethnoracial categories across the groups; patients in the AD group were white while the controls were more diverse.

In all, this study found that pathways related to transmethylation, antioxidant capacity, and energy regulation are reduced in postmortem AD compared to controls. These differences were diminished when CeVD was present in the control and AD groups. Our findings point to AD-specific changes in transmethylation, antioxidant and energy metabolism pathways that could be explored as future drug targets.

Conflicts of Interest: None to declare

Author Contributions: D.A.S. and A.Y.T. conceived the study. D.A.S. prepared sample extracts for NMR, analyzed acquired spectra, and prepared the manuscript. Y.O. prepared sample extracts from tissue samples. B.N.D. and L.W.J. performed the clinical pathology diagnosis for AD and control cases, oversaw case selection, dissected samples, and provided critical review of the manuscript. C.M.S. assisted in acquiring NMR spectra. D.J.H. assisted with the statistical analysis and interpretation of the statistical results. A.Y.T. assisted with data and statistical analysis and manuscript preparation. All authors reviewed the manuscript.

Funding: The authors are indebted to the families and participants of the UCD ADRC for their generous donations. Research reported in this publication was supported by the Alzheimer's Association (2018-AARGD-591676) and the National Institute On Aging of the National Institutes of Health under Award Number P30AG010129.

Table 1: Descriptive statistics for patient cohort in Alzheimer's Disease (AD), Control, Alzheimer's Disease with Cerebrovascular Disease (AD+CeVD), and Controls with Cerebrovascular Disease (Control+CeVD). Values that do not share a common superscript differ ($p < 0.05$).

	Control	Control+CeVD	AD	AD+CeVD	P value
N	16	4	15	6	n/a
Sex	8 female, 8 male	2 male, 2 female	10 female, 5 male	2 female, 4 male	0.573
Ethnicity	9 White, 4 Hispanic, 2 African/American, 1 American Indian/Alaskan Native	1 African/American, 1 White, 1 Asian, 1 Hispanic	15 White	6 White	n/a
Age at death, (yrs)	81.1±9.2	85.0±5.8	81.5±7.3	87.5±3.4	0.304
Post-mortem interval (hrs.)	24.3±32.3	24.4±32.3	7.5±4.9	19.3±17.9	0.122
Braak NFT stage (mean, SD)	1.7 ± 0.5^{b}	1.3 ± 0.5^{b}	5.8 ± 0.40^{a}	5.8 ± 0.4^{a}	<0.0001

Table 2: Log-transformed means and standard deviations of brain concentrations of metabolites that significantly differ (glutathione, 2-hydroxybutyrate, fumarate, and sarcosine) by multiple regression analysis between controls and AD both with and without CeVD. Data are expressed as mean±SD in units of $\log_{10}(\frac{\text{nmol}}{\text{g brain}})$.

Analyte	**Control**	**Control+CeVD**	**AD**	**AD+CeVD**
2-Hydroxybutyrate	1.32±0.51	1.50±0.16	1.49±0.36	1.36±0.64
Glutathione	1.63±0.30	1.47±0.27	1.54±0.30	1.32±0.39
Fumarate	1.01±0.35	0.89±0.30	0.89±0.39	0.88±0.50
Sarcosine	1.00±0.45	1.04±0.35	0.72±0.39	1.18±0.33

Table 3: Significant results of multiple regression analysis. For each variable (intercept, group effects, CeVD effects, PMI, Age, and second order effects between Group and CeVD, PMI, and age) results are represented as Estimate ± standard error (95% confidence interval) and are marked with an asterisk (*) if the effect was significant.

Analyte	**Intercept**	**Group**	**CeVD**	**PMI**	**Age**	**Group:CeVD**	**Group:PMI**	**Group:Age**
2-hydroxy-butyrate	1.327±0.106 (1.111,1.542)*	-0.165±0.187 (-0.545,0.215)	0.137±0.244 (-0.360,0.633)	0.006±0.012 (-0.017,0.030)	0.001±0.003 (-0.005,0.007)	0.234±0.346 (-0.471,0.939)	-0.040±0.188 (-0.079,-0.002)*	-0.026±0.010 (-0.047,-0.006)*
Glutathione	1.658±0.067 (1.522,1.793)*	-0.298±1.118 (-0.537,-0.059)*	-0.100±0.154 (-0.412,0.212)	0.002±0.007 (-0.013,0.016)	-0.004±0.002 (-0.008,-0.001)*	0.188±0.218 (-0.255,0.632)	-0.026±0.012 (-0.050,-0.002)*	-0.009±0.006 (-0.022,0.004)
Fumarate	1.029±0.091 (0.843,1.215)*	-0.379±0.161 (-0.707,-0.052)*	-0.042±0.210 (-0.470,0.385)	-0.001±0.010 (-0.022,0.019)	-0.004±0.002 (-0.009,0.001)	0.298±0.298 (-0.309,0.905)	-0.002±0.016 (-0.035,0.031)	-0.016±0.009 (-0.034,0.001)
Sarcosine	1.042±0.099 (0.840,1.244)*	-0.400±0.175 (-0.756,-0.043)*	-0.031±0.229 (-0.497±0.435)	0.025±0.011 (0.002,0.047)*	-0.001±0.003 (-0.007,0.004)	0.546±0.325 (-0.115,1.208)	-0.020±0.018 (-0.056,0.016)	-0.006±0.009 (-0.025,0.014)

Supplementary Table 1: All patient information including age at death, sex, and BRAAK NFT stage.

Case ID	Group	Age at Death (yrs)	Sex	Ethnicity	PMI (hrs)	BRAAK NFT stage
1	Control	77	M	White	6	1
2	Control	90+	M	Hispanic	7	2
3	Control	84	F	White	13.1	1
4	Control	90+	F	African/American	7	2
5	Control	76	F	White	107	2
6	Control	78	F	White	48	2
7	Control	65	F	White	8	1
8	Control	90+	F	White	1	2
9	Control	90+	F	Amer Indian/Alaskan Native	4	2
10	Control	90+	M	African/American	7	1
11	Control+CeVD	81	M	African/American	115	1
12	Control+CeVD	90+	M	White	3.5	1
13	Control+CeVD	90+	F	Asian	40	1
14	Control	90+	F	White	7	2
15	Control	75	M	Hispanic	88	2
16	Control	75	M	Hispanic	50	2
17	Control	90+	M	Hispanic	22	1
18	Control+CeVD	79	F	Hispanic	4	2
19	Control	66	M	White	12	2
20	Control	71	M	White	3	2
21	AD	86	F	White	1	6
22	AD	89	F	White	2	6
23	AD	74	M	White	8	6
24	AD	90+	F	White	11	6
25	AD+CeVD	90+	M	White	13	6
26	AD	87	F	White	11	6
27	AD+CeVD	89	F	White	35	6
28	AD	86	F	White	3	6
29	AD	79	M	White	4	6
30	AD	88	F	White	11	5
31	AD	79	M	White	5	6
32	AD	71	M	White	9	6
33	AD	90+	F	White	9	6
34	AD+CeVD	87	F	White	8	5
35	AD+CeVD	88	M	White	7	6
36	AD	85	M	White	4	5
37	AD+CeVD	81	M	White	5	6
38	AD+CeVD	90+	M	White	48	6
39	AD	70	F	White	10	6
40	AD	77	F	White	5	6
41	AD	72	F	White	20	5

Supplementary Table 2: Log-transformed metabolite concentrations (nmol/g brain) for all metabolites measured. Metabolites that were not detected are marked as ND. Data are expressed as mean±SD in units of $\log_{10}(\frac{\text{nmol}}{\text{g brain}})$.

Analyte	Control	Control + CeVD	AD	AD + CeVD
2-Hydroxybutyrate	1.32±0.51	1.50±0.16	1.49±0.36	1.36±0.64
3-Hydroxybutyrate	1.49±0.62	1.59±0.39	1.52±0.35	1.39±0.35
3-Hydroxyisovalerate	ND	ND	ND	ND
4-Aminobutyrate	2.37±0.33	2.40±0.35	2.49±0.23	2.30±0.46
ADP	0.88±0.48	1.03±0.25	1.06±0.32	0.64±0.44
AMP	1.23±0.54	1.04±0.44	1.25±0.48	1.09±0.49
ATP	0.91±0.45	1.06±0.38	1.12±0.23	0.85±0.45
Acetate	2.62±0.39	2.56±0.16	2.67±0.34	2.56±0.31
Acetoacetate	0.72±0.35	0.71±0.42	0.69±0.23	0.40±0.37
Acetone	0.60±0.38	0.43±0.50	0.58±0.38	0.47±0.51
Adenosine	ND	ND	ND	ND
Alanine	2.60±0.38	2.63±0.22	2.77±0.30	2.66±0.36
Ascorbate	ND	ND	ND	ND
Aspartate	2.71±0.44	2.77±0.22	2.80±0.32	2.64±0.40
Benzoate	ND	ND	ND	ND
Carnitine	1.86±0.27	1.74±0.25	1.88±0.25	1.67±0.26
Carnosine	1.49±0.40	1.40±0.17	1.56±0.42	1.54±0.18
Choline	1.93±0.42	1.94±0.18	1.80±0.33	1.78±0.27
Creatine	3.29±0.41	3.30±0.29	3.42±0.28	3.27±0.41
Creatine phosphate	1.88±0.36	1.96±0.15	1.97±0.26	1.92±0.40
Dimethyl sulfone	ND	ND	ND	ND
Ethanol	ND	ND	ND	ND
Formate	2.21±0.30	2.23±0.30	2.35±0.27	2.25±0.33
Fumarate	1.01±0.35	0.89±0.30	0.89±0.39	0.88±0.50
GTP	1.13±0.61	0.96±0.53	1.23±0.25	0.92±0.79
Glucose	1.82±0.56	1.55±0.68	1.93±0.69	1.70±0.80
Glucose-6-phosphate	ND	ND	ND	ND
Glutamate	3.34±0.37	3.42±0.33	3.47±0.29	3.29±0.50
Glutamine	3.09±0.41	3.13±0.36	3.29±0.35	3.06±0.54
Glutathione	1.63±0.30	1.47±0.27	1.54±0.30	1.32±0.39
Glycine	2.31±0.27	2.60±0.20	2.44±0.31	2.35±0.35
Histidine	1.46±0.29	1.43±0.32	1.56±0.27	1.59±0.21
Hypoxanthine	2.08±0.59	1.97±0.29	2.19±0.41	2.04±0.39
IMP	0.81±0.29	0.78±0.15	0.67±0.30	0.75±0.40
Inosine	2.13±0.45	2.10±0.37	2.32±0.29	2.09±0.52
Isoleucine	1.79±0.45	1.91±0.17	1.99±0.34	1.92±0.32

Isovalerate	0.05±0.35	0.31±0.33	0.23±0.38	0.04±0.24
Lactate	3.85±0.37	3.85±0.29	4.01±0.27	3.87±0.43
Leucine	2.06±0.43	2.18±0.14	2.27±0.32	2.19±0.33
Lysine	1.88±0.32	1.85±0.24	1.85±0.32	1.80±0.40
Methanol	2.91±0.25	2.93±0.19	2.97±0.28	2.93±0.27
N-Acetylaspartate	3.08±0.38	3.01±0.39	3.14±0.25	2.97±0.45
NAD+	0.54±0.47	0.61±0.37	0.60±0.47	0.45±0.44
NADH	ND	ND	ND	ND
Nicotinurate	1.22±0.31	1.18±0.34	1.25±0.27	1.20±0.31
O-Acetylcholine	1.68±0.41	1.82±0.19	1.85±0.36	1.86±0.35
O-Phosphocholine	2.17±0.42	2.17±0.13	2.37±0.37	2.18±0.45
Pantothenate	0.99±0.49	1.05±0.18	1.05±0.36	0.89±0.39
Phenylalanine	1.82±0.38	1.88±0.23	2.02±0.37	1.91±0.44
Propylene glycol	1.20±0.31	1.36±0.41	1.23±0.35	1.45±0.34
Sarcosine	1.00±0.45	1.04±0.35	0.72±0.39	1.18±0.33
Succinate	2.09±0.44	2.19±0.23	2.30±0.29	2.11±0.43
Taurine	2.50±0.43	2.45±0.27	2.57±0.32	2.43±0.51
Threonine	2.05±0.32	2.15±0.15	2.16±0.30	2.06±0.37
Tryptophan	1.18±0.40	1.23±0.37	1.24±0.43	1.37±0.42
Tyrosine	1.91±0.41	1.99±0.24	2.09±0.38	2.00±0.42
UDP-N-Acetylglucosamine	0.90±0.35	0.83±0.40	0.90±0.30	1.00±0.38
UMP	ND	ND	ND	ND
Uracil	1.25±0.50	1.04±0.29	1.27±0.44	1.18±0.36
Urea	3.50±0.42	3.60±0.26	3.55±0.46	3.87±0.36
Valine	2.00±0.47	2.17±0.18	2.23±0.33	2.15±0.35
myo-Inositol	3.24±0.47	3.20±0.25	3.42±0.30	3.28±0.47
sn-Glycero-3-phosphocholine	2.45±0.60	2.58±0.51	2.72±0.31	2.63±0.56

Conclusion

The work of this thesis indicates that ischemia and brain dissection are significant problems when performing postmortem metabolomic studies. In Study 1, we found both the ischemia that occurs postmortem as well as the brain dissection process matters, as many metabolites changed within the six minute postmortem period. These include changes in phosphorylation through the depletion of high energy phosphate metabolites such as phosphocreatine and adenosine triphosphate (ATP), the buildup of lactate, and the depletion of glucose. We also observed increases in antioxidants following hypercapnia/ischemia, which decreased back to levels seen in controls that received microwave irradiation. We observed *sn*-3 glycerophosphocholine to decrease while choline increased, suggesting changes in lipid turnover. The branched chain amino acids isoleucine, leucine, and valine, as well as histidine and tyrosine were significantly elevated in the group that received only CO_2 compared to controls. In Study 2, we found differences in a handful of metabolites (sarcosine, fumarate and glutathione) between Alzheimer's Disease (AD) without Cerebrovascular Disease (CeVD) and controls without CeVD only emerged when controlling for the postmortem interval and age. It is likely that the effects from the postmortem interval and agonal state diminished further metabolomic effects associated with AD.

There were several limitations to this thesis. The first of these is that we did not control the temperature of the rats in Study 1. Hypothermia has been shown to decrease concentrations of glutamate and leucine, and increase the concentration of γ-aminobutyric acid (GABA)[160]. During death, the loss of blood flow to the brain reduces availability of oxygen, which leads to a buildup of CO_2 in the brain. This is accompanied by a reduction in consumption of oxygen and shift towards anaerobic metabolism[161]. In humans, algor mortis (i.e. the cooling of the body after

death) sets in approximately 30 minutes after death, after which the body cools at a rate of approximately 1ºC per hour for the first twelve hours, and approximately 0.5ºC per hour thereafter[162] until it reaches ambient temperature. Most decedents are stored in refrigerated conditions at temperatures of between 2ºC and 4ºC[163]. As rats are smaller than humans, this heat loss is likely much faster although this is understudied.

The first two groups in Study 1, which received microwave irradiation and CO_2 followed by immediate microwave irradiation respectively are unlikely to be affected by hypothermia since the animals died immediately after head-focused microwave irradiation (algor mortis only occur postmortem). This represents a potential confounding factor for Groups 3 and 4, which were decapitated and subjected for a 6 minute wait period to induce prolonged ischemia (Group 3) or dissected within 6 minutes (Group 4). While some metabolites, such as ATP and phosphocreatine likely were not affected significantly by this hypothermia[116], it remains possible that some of the metabolites that changed due to dissection, such as UDP-N-acetylglucosamine, leucine, isoleucine, or phenylalanine were influenced by hypothermia. The effects of algor mortis could be limited in a future study by using a heating pad during CO_2 euthanasia.

An additional limitation of Study 1 was that Group 2 received microwave irradiation immediately after exposure to CO_2 for 2-minutes, and it was not conclusively determined whether the rat had died during this 2-minute period. Death would result in postmortem ischemia (versus hypercapnia) which would alter concentrations of brain metabolites. Additionally, there is the possibility that two rats in Group 1 (which received microwave irradiation) were not properly microwaved, as in the PCA plot (Figure 1, Chapter 2), two rats clustered with Groups 2 and 3 (CO_2+MW and CO_2+Wait+MW).

Further, in Study 1 only male rats were evaluated. This was done as the evaluation of small metabolites was a secondary analysis, and the primary analysis[101] was conceived to replicate changes in oxidized lipids that other authors had observed in males[99,164-167]. Future studies should investigate sex differences in the response to hypercapnia/ischemia and dissection.

Another major limitation of this thesis is that rats do not completely mimic the human condition. Metabolites that we observed to change in the six minutes postmortem in rats may change differently or not at all in humans. For example, the half-life of glucose in the rat brain is approximately 1.6 minutes[168] while the half-life of glucose in the human brain has been measured to be between 2 and 4 minutes[169,170]. We only measured six minutes of ischemia in Study 1, whereas in Study 2 the postmortem interval (PMI) for patients in both groups was orders of magnitude larger. The effects of longer-term ischemia could be investigated by including an additional group subjected to hours of postmortem ischemia to represent the average time prior to dissection that a human brain receives. However, due to differences in metabolism between rats and humans, the applicability of this approach would be limited only to metabolites whose half-lives are comparable between rats and humans in the timeframe studied. To exemplify, docosahexaenoic acid, has a half-life of 30-90 days in rats[171] and approximately 2.5 years in humans[172].

Additionally, the human tissue studied in Study 2 underwent more freeze-thaw cycles than the rat brain tissue studied in Study 1. Where the tissue from Study 1 only went through a single freeze-thaw cycle before metabolomic analysis, the tissue from Study 2 went through at least two. The effects of freeze-thawing could be investigated with an experiment in which CO_2-asphyxiated and microwave irradiated rats are subjected to repeated freeze-thaw cycles, with one group receiving only a single cycle, a second group receiving two, and a third group receiving as

many as three. Lastly, the agonal state that humans undergo pre-death is difficult to model in animals and cannot be adequately captured or statistically controlled for in human cohort studies.

This leaves positron emission tomography (PET) imaging as the most obvious option to simply perform metabolomic studies *in vivo* (. Regional evaluation of metabolites could be performed using PET; however, this methodology is limited by a lack of availability of appropriate tracers, only one of which can be used at a time, and regional resolution (when compared to pathology). Additionally, some studies have indicated that due to the limited ability for many tracers to cross the blood-brain barrier, it is generally more effective to study compounds that enter the brain via passive diffusion, such as free fatty acids[173] than compounds that must enter the brain via active or coupled transport.

A major limitation of Study 2 is that the analysis was restricted to one brain region (pre-frontal cortex). We evaluated metabolite concentrations within the prefrontal cortex, because it is affected by AD pathology late into the progression of the disease[6]. This could be one of the reasons as to why we did not see many of the metabolomic changes that other authors such as Mahajan observed[27,95], as their study evaluated concentrations in regions that are affected earlier in the disease- potentially suggesting these metabolic changes, which are localized to the brain region studied, do not develop instantaneously and build up over time as more cells become affected by AD pathology. A postmortem study evaluating multiple brain regions including the prefrontal cortex, inferior temporal gyrus, middle frontal gyrus, and also the cerebellum, which is one of the last regions of the brain to be affected[6], would allow for a more comprehensive mapping of metabolomic changes in AD.

It is possible that one reason we did not see any differences in the CeVD groups in Study 2 was because of the small sample size of patients with a CeVD diagnosis in the control and AD

groups. Our statistical model likely did not have the power or effect size to determine if there were any differences in between CeVD and the control groups ,and this could be remedied by including a larger cohort.

In conclusion, this thesis was able to differentiate the effects of postmortem ischemia from the changes imposed due to the dissection of the brain, by comparing microwave irradiation to CO_2 asphyxiation followed by immediate microwave irradiation, to CO_2 asphyxiation followed by a simulated dissection time and subsequent microwave irradiation, and to CO_2 asphyxiation and dissection (no microwave irradiation) in Study 1. Additionally, Study 1 identified metabolites that are stable within 6 minutes of postmortem dissection, and metabolites that are not. However, caution should be exercised when extrapolating these results to a human PMI, which is typically measured on the magnitude of hours, and because metabolic turnover of these metabolites may be different in rats than it is in humans. Knowing that the PMI matters, Study 2 was able to take that into account and still find significant differences between the AD and control subjects. Many studies[95] simply match postmortem intervals between groups, whereas we were able to statistically control for it and therefore minimize its effects. Additionally, we also considered the effects of vascular disease (i.e. CeVD), which involves a more chronic and subtle state of localized ischemia within the brain. Few studies consider heterogeneous presentations of AD in their analyses, although in doing so, we did not observe any significant effects in CeVD with or without AD with our current sample size, though we were able to highlight changes in several metabolites in AD without CeVD. Further, the postmortem brains in Study 2 had confirmed pathological diagnoses which strengthens the validity of our observations.

In all, this thesis found that the postmortem effects of ischemia and dissection affects the brain metabolome. This may obscure or limit potential changes related to vascular disease and AD pathology in humans. Postmortem studies should consider the confounding effects of PMI rather than matching PMI between groups since many metabolites likely change depending on the PMI.

REFERENCES

1 About a peculiar disease of the cerebral cortex. By Alois Alzheimer, 1907 (Translated by L. Jarvik and H. Greenson). *Alzheimer Dis Assoc Disord* **1**, 3-8 (1987).

2 Mayeux, R. & Stern, Y. Epidemiology of Alzheimer disease. *Cold Spring Harb Perspect Med* **2**, doi:10.1101/cshperspect.a006239 (2012).

3 Unnithan, A. K. A. & Mehta, P. in *StatPearls* (2021).

4 WHO. *Dementia*, <https://www.who.int/news-room/fact-sheets/detail/dementia> (2020).

5 Alonso, A. C., Grundke-Iqbal, I. & Iqbal, K. Alzheimer's disease hyperphosphorylated tau sequesters normal tau into tangles of filaments and disassembles microtubules. *Nat Med* **2**, 783-787, doi:10.1038/nm0796-783 (1996).

6 Braak, H. & Braak, E. Neuropathological stageing of Alzheimer-related changes. *Acta Neuropathol* **82**, 239-259, doi:10.1007/BF00308809 (1991).

7 Park, K. H. J. & Barrett, T. Gliosis Precedes Amyloid-beta Deposition and Pathological Tau Accumulation in the Neuronal Cell Cycle Re-Entry Mouse Model of Alzheimer's Disease. *J Alzheimers Dis Rep* **4**, 243-253, doi:10.3233/ADR-200170 (2020).

8 Schneider, J. A., Arvanitakis, Z., Bang, W. & Bennett, D. A. Mixed brain pathologies account for most dementia cases in community-dwelling older persons. *Neurology* **69**, 2197-2204, doi:10.1212/01.wnl.0000271090.28148.24 (2007).

9 Thal, D. R. & Braak, H. [Post-mortem diagnosis of Alzheimer's disease]. *Pathologe* **26**, 201-213, doi:10.1007/s00292-004-0695-4 (2005).

10 Lim, A. *et al.* Clinico-neuropathological correlation of Alzheimer's disease in a community-based case series. *J Am Geriatr Soc* **47**, 564-569, doi:10.1111/j.1532-5415.1999.tb02571.x (1999).

11 Thal, D. R., Rub, U., Orantes, M. & Braak, H. Phases of A beta-deposition in the human brain and its relevance for the development of AD. *Neurology* **58**, 1791-1800, doi:10.1212/wnl.58.12.1791 (2002).

12 Mirra, S. S. *et al.* The Consortium to Establish a Registry for Alzheimer's Disease (CERAD). Part II. Standardization of the neuropathologic assessment of Alzheimer's disease. *Neurology* **41**, 479-486, doi:10.1212/wnl.41.4.479 (1991).

13 Zimmerman, H. M. *Progress in Neuropathology*. 1-26 (Grune & Stratton, 1973).

14 Alafuzoff, I. *et al.* Staging of neurofibrillary pathology in Alzheimer's disease: a study of the BrainNet Europe Consortium. *Brain Pathol* **18**, 484-496, doi:10.1111/j.1750-3639.2008.00147.x (2008).

15 Montine, T. J. *et al.* National Institute on Aging-Alzheimer's Association guidelines for the neuropathologic assessment of Alzheimer's disease: a practical approach. *Acta Neuropathol* **123**, 1-11, doi:10.1007/s00401-011-0910-3 (2012).

16 Serrano-Pozo, A. *et al.* Thal Amyloid Stages Do Not Significantly Impact the Correlation Between Neuropathological Change and Cognition in the Alzheimer Disease Continuum. *J Neuropathol Exp Neurol* **75**, 516-526, doi:10.1093/jnen/nlw026 (2016).

17 Curtis, D. R. & Watkins, J. C. The excitation and depression of spinal neurones by structurally related amino acids. *J Neurochem* **6**, 117-141, doi:10.1111/j.1471-4159.1960.tb13458.x (1960).

18 Ding, X. *et al.* Silencing IFN-gamma binding/signaling in astrocytes versus microglia leads to opposite effects on central nervous system autoimmunity. *J Immunol* **194**, 4251-4264, doi:10.4049/jimmunol.1303321 (2015).

19 Games, D. *et al.* Alzheimer-type neuropathology in transgenic mice overexpressing V717F beta-amyloid precursor protein. *Nature* **373**, 523-527, doi:10.1038/373523a0 (1995).

20 Heneka, M. T. *et al.* Induction of nitric oxide synthase and nitric oxide-mediated apoptosis in neuronal PC12 cells after stimulation with tumor necrosis factor-alpha/lipopolysaccharide. *J Neurochem* **71**, 88-94, doi:10.1046/j.1471-4159.1998.71010088.x (1998).
21 Lesne, S. *et al.* A specific amyloid-beta protein assembly in the brain impairs memory. *Nature* **440**, 352-357, doi:10.1038/nature04533 (2006).
22 Mandelkow, E. M. & Mandelkow, E. Biochemistry and cell biology of tau protein in neurofibrillary degeneration. *Cold Spring Harb Perspect Med* **2**, a006247, doi:10.1101/cshperspect.a006247 (2012).
23 Pinessi, L. *et al.* Biogenic amines in cerebrospinal fluid and plasma of patients with dementia of Alzheimer type. *Funct Neurol* **2**, 51-58 (1987).
24 Tan, J. *et al.* Microglial activation resulting from CD40-CD40L interaction after beta-amyloid stimulation. *Science* **286**, 2352-2355, doi:10.1126/science.286.5448.2352 (1999).
25 Tohgi, H., Ueno, M., Abe, T., Takahashi, S. & Nozaki, Y. Concentrations of monoamines and their metabolites in the cerebrospinal fluid from patients with senile dementia of the Alzheimer type and vascular dementia of the Binswanger type. *J Neural Transm Park Dis Dement Sect* **4**, 69-77, doi:10.1007/BF02257623 (1992).
26 Volicer, L., Langlais, P. J., Matson, W. R., Mark, K. A. & Gamache, P. H. Serotoninergic system in dementia of the Alzheimer type. Abnormal forms of 5-hydroxytryptophan and serotonin in cerebrospinal fluid. *Arch Neurol* **42**, 1158-1161, doi:10.1001/archneur.1985.04060110040013 (1985).
27 An, Y. *et al.* Evidence for brain glucose dysregulation in Alzheimer's disease. *Alzheimers Dement* **14**, 318-329, doi:10.1016/j.jalz.2017.09.011 (2018).
28 Chen, F. *et al.* TMP21 is a presenilin complex component that modulates gamma-secretase but not epsilon-secretase activity. *Nature* **440**, 1208-1212, doi:10.1038/nature04667 (2006).
29 Nistor, M. *et al.* Alpha- and beta-secretase activity as a function of age and beta-amyloid in Down syndrome and normal brain. *Neurobiol Aging* **28**, 1493-1506, doi:10.1016/j.neurobiolaging.2006.06.023 (2007).
30 Driscoll, I. & Troncoso, J. Asymptomatic Alzheimer's disease: a prodrome or a state of resilience? *Curr Alzheimer Res* **8**, 330-335, doi:10.2174/156720511795745348 (2011).
31 Elder, G. A., Gama Sosa, M. A. & De Gasperi, R. Transgenic mouse models of Alzheimer's disease. *Mt Sinai J Med* **77**, 69-81, doi:10.1002/msj.20159 (2010).
32 Hsiao, K. *et al.* Correlative memory deficits, Abeta elevation, and amyloid plaques in transgenic mice. *Science* **274**, 99-102, doi:10.1126/science.274.5284.99 (1996).
33 Duff, K. *et al.* Increased amyloid-beta42(43) in brains of mice expressing mutant presenilin 1. *Nature* **383**, 710-713, doi:10.1038/383710a0 (1996).
34 Nilsson, P., Saito, T. & Saido, T. C. New mouse model of Alzheimer's. *ACS Chem Neurosci* **5**, 499-502, doi:10.1021/cn500105p (2014).
35 Stamer, K., Vogel, R., Thies, E., Mandelkow, E. & Mandelkow, E. M. Tau blocks traffic of organelles, neurofilaments, and APP vesicles in neurons and enhances oxidative stress. *J Cell Biol* **156**, 1051-1063, doi:10.1083/jcb.200108057 (2002).
36 Arriagada, P. V., Growdon, J. H., Hedley-Whyte, E. T. & Hyman, B. T. Neurofibrillary tangles but not senile plaques parallel duration and severity of Alzheimer's disease. *Neurology* **42**, 631-639, doi:10.1212/wnl.42.3.631 (1992).
37 Hayashi, S. *et al.* Late-onset frontotemporal dementia with a novel exon 1 (Arg5His) tau gene mutation. *Ann Neurol* **51**, 525-530, doi:10.1002/ana.10163 (2002).
38 Poorkaj, P. *et al.* An R5L tau mutation in a subject with a progressive supranuclear palsy phenotype. *Ann Neurol* **52**, 511-516, doi:10.1002/ana.10340 (2002).

39 Lee, V. M., Kenyon, T. K. & Trojanowski, J. Q. Transgenic animal models of tauopathies. *Biochim Biophys Acta* **1739**, 251-259, doi:10.1016/j.bbadis.2004.06.014 (2005).
40 Goedert, M., Spillantini, M. G., Jakes, R., Rutherford, D. & Crowther, R. A. Multiple isoforms of human microtubule-associated protein tau: sequences and localization in neurofibrillary tangles of Alzheimer's disease. *Neuron* **3**, 519-526, doi:10.1016/0896-6273(89)90210-9 (1989).
41 Ishihara, T. *et al.* Age-dependent emergence and progression of a tauopathy in transgenic mice overexpressing the shortest human tau isoform. *Neuron* **24**, 751-762, doi:10.1016/s0896-6273(00)81127-7 (1999).
42 Morsch, R., Simon, W. & Coleman, P. D. Neurons may live for decades with neurofibrillary tangles. *J Neuropathol Exp Neurol* **58**, 188-197, doi:10.1097/00005072-199902000-00008 (1999).
43 Gomez-Isla, T. *et al.* Neuronal loss correlates with but exceeds neurofibrillary tangles in Alzheimer's disease. *Ann Neurol* **41**, 17-24, doi:10.1002/ana.410410106 (1997).
44 Takeda, A. *et al.* In Alzheimer's disease, heme oxygenase is coincident with Alz50, an epitope of tau induced by 4-hydroxy-2-nonenal modification. *J Neurochem* **75**, 1234-1241, doi:10.1046/j.1471-4159.2000.0751234.x (2000).
45 Dujardin, S. *et al.* Different tau species lead to heterogeneous tau pathology propagation and misfolding. *Acta Neuropathol Commun* **6**, 132, doi:10.1186/s40478-018-0637-7 (2018).
46 Honig, L. S. *et al.* Trial of Solanezumab for Mild Dementia Due to Alzheimer's Disease. *N Engl J Med* **378**, 321-330, doi:10.1056/NEJMoa1705971 (2018).
47 Salloway, S. *et al.* A trial of gantenerumab or solanezumab in dominantly inherited Alzheimer's disease. *Nat Med* **27**, 1187-1196, doi:10.1038/s41591-021-01369-8 (2021).
48 Vlassenko, A. G. *et al.* Amyloid-beta plaque growth in cognitively normal adults: longitudinal [11C]Pittsburgh compound B data. *Ann Neurol* **70**, 857-861, doi:10.1002/ana.22608 (2011).
49 Crews, L., Patrick, C., Adame, A., Rockenstein, E. & Masliah, E. Modulation of aberrant CDK5 signaling rescues impaired neurogenesis in models of Alzheimer's disease. *Cell Death Dis* **2**, e120, doi:10.1038/cddis.2011.2 (2011).
50 Gauthier, S. *et al.* Efficacy and safety of tau-aggregation inhibitor therapy in patients with mild or moderate Alzheimer's disease: a randomised, controlled, double-blind, parallel-arm, phase 3 trial. *Lancet* **388**, 2873-2884, doi:10.1016/S0140-6736(16)31275-2 (2016).
51 Dumuis, A., Sebben, M., Haynes, L., Pin, J. P. & Bockaert, J. NMDA receptors activate the arachidonic acid cascade system in striatal neurons. *Nature* **336**, 68-70, doi:10.1038/336068a0 (1988).
52 Gardiner, M., Nilsson, B., Rehncrona, S. & Siesjo, B. K. Free fatty acids in the rat brain in moderate and severe hypoxia. *J Neurochem* **36**, 1500-1505, doi:10.1111/j.1471-4159.1981.tb00592.x (1981).
53 Lim, G. P. *et al.* Ibuprofen suppresses plaque pathology and inflammation in a mouse model for Alzheimer's disease. *J Neurosci* **20**, 5709-5714 (2000).
54 Abbas, N. *et al.* Up-regulation of the inflammatory cytokines IFN-gamma and IL-12 and down-regulation of IL-4 in cerebral cortex regions of APP(SWE) transgenic mice. *J Neuroimmunol* **126**, 50-57, doi:10.1016/s0165-5728(02)00050-4 (2002).
55 Deutsch, J. A. The cholinergic synapse and the site of memory. *Science* **174**, 788-794, doi:10.1126/science.174.4011.788 (1971).
56 Drachman, D. A. & Leavitt, J. Human memory and the cholinergic system. A relationship to aging? *Arch Neurol* **30**, 113-121, doi:10.1001/archneur.1974.00490320001001 (1974).
57 Bowen, D. M., Smith, C. B., White, P. & Davison, A. N. Neurotransmitter-related enzymes and indices of hypoxia in senile dementia and other abiotrophies. *Brain* **99**, 459-496, doi:10.1093/brain/99.3.459 (1976).

58 Rodriguez, G. *et al.* Quantitative EEG changes in Alzheimer patients during long-term donepezil therapy. *Neuropsychobiology* **46**, 49-56, doi:10.1159/000063576 (2002).
59 Findley, C. A., Bartke, A., Hascup, K. N. & Hascup, E. R. Amyloid Beta-Related Alterations to Glutamate Signaling Dynamics During Alzheimer's Disease Progression. *ASN Neuro* **11**, 1759091419855541, doi:10.1177/1759091419855541 (2019).
60 Hascup, K. N., Findley, C. A., Sime, L. N. & Hascup, E. R. Hippocampal alterations in glutamatergic signaling during amyloid progression in AbetaPP/PS1 mice. *Sci Rep* **10**, 14503, doi:10.1038/s41598-020-71587-6 (2020).
61 Tanaka, K. *et al.* Epilepsy and exacerbation of brain injury in mice lacking the glutamate transporter GLT-1. *Science* **276**, 1699-1702, doi:10.1126/science.276.5319.1699 (1997).
62 Jacob, C. P. *et al.* Alterations in expression of glutamatergic transporters and receptors in sporadic Alzheimer's disease. *J Alzheimers Dis* **11**, 97-116, doi:10.3233/jad-2007-11113 (2007).
63 Wenk, G. L., Parsons, C. G. & Danysz, W. Potential role of N-methyl-D-aspartate receptors as executors of neurodegeneration resulting from diverse insults: focus on memantine. *Behav Pharmacol* **17**, 411-424, doi:10.1097/00008877-200609000-00007 (2006).
64 FDA. (2005).
65 Soininen, H., MacDonald, E., Rekonen, M. & Riekkinen, P. J. Homovanillic acid and 5-hydroxyindoleacetic acid levels in cerebrospinal fluid of patients with senile dementia of Alzheimer type. *Acta Neurol Scand* **64**, 101-107, doi:10.1111/j.1600-0404.1981.tb04392.x (1981).
66 Bareggi, S. R., Franceschi, M., Bonini, L., Zecca, L. & Smirne, S. Decreased CSF concentrations of homovanillic acid and gamma-aminobutyric acid in Alzheimer's disease. Age- or disease-related modifications? *Arch Neurol* **39**, 709-712, doi:10.1001/archneur.1982.00510230035010 (1982).
67 Zimmer, R. *et al.* Gamma-aminobutyric acid and homovanillic acid concentration in the CSF of patients with senile dementia of Alzheimer's type. *Arch Neurol* **41**, 602-604, doi:10.1001/archneur.1984.04210080010005 (1984).
68 Chi, S. *et al.* The prevalence of depression in Alzheimer's disease: a systematic review and meta-analysis. *Curr Alzheimer Res* **12**, 189-198, doi:10.2174/1567205012666150204124310 (2015).
69 Rosenberg, P. B. *et al.* Sertraline for the treatment of depression in Alzheimer disease. *Am J Geriatr Psychiatry* **18**, 136-145, doi:10.1097/JGP.0b013e3181c796eb (2010).
70 Ravaglia, G. *et al.* Prevalent depressive symptoms as a risk factor for conversion to mild cognitive impairment in an elderly Italian cohort. *Am J Geriatr Psychiatry* **16**, 834-843, doi:10.1097/JGP.0b013e318181f9b1 (2008).
71 Schneider, J. A., Aggarwal, N. T., Barnes, L., Boyle, P. & Bennett, D. A. The neuropathology of older persons with and without dementia from community versus clinic cohorts. *J Alzheimers Dis* **18**, 691-701, doi:10.3233/JAD-2009-1227 (2009).
72 Klatka, L. A., Schiffer, R. B., Powers, J. M. & Kazee, A. M. Incorrect diagnosis of Alzheimer's disease. A clinicopathologic study. *Arch Neurol* **53**, 35-42, doi:10.1001/archneur.1996.00550010045015 (1996).
73 Kuzma, E. *et al.* Stroke and dementia risk: A systematic review and meta-analysis. *Alzheimers Dement* **14**, 1416-1426, doi:10.1016/j.jalz.2018.06.3061 (2018).
74 Cairns, N. J. *et al.* TDP-43 in familial and sporadic frontotemporal lobar degeneration with ubiquitin inclusions. *Am J Pathol* **171**, 227-240, doi:10.2353/ajpath.2007.070182 (2007).
75 Rademakers, R., Cruts, M. & van Broeckhoven, C. The role of tau (MAPT) in frontotemporal dementia and related tauopathies. *Hum Mutat* **24**, 277-295, doi:10.1002/humu.20086 (2004).
76 Kertesz, A. *et al.* Familial frontotemporal dementia with ubiquitin-positive, tau-negative inclusions. *Neurology* **54**, 818-827, doi:10.1212/wnl.54.4.818 (2000).

77 McCarron, M. O., Delong, D. & Alberts, M. J. APOE genotype as a risk factor for ischemic cerebrovascular disease: a meta-analysis. *Neurology* **53**, 1308-1311, doi:10.1212/wnl.53.6.1308 (1999).
78 Dublin, S. *et al.* Atrial fibrillation and risk of dementia: a prospective cohort study. *J Am Geriatr Soc* **59**, 1369-1375, doi:10.1111/j.1532-5415.2011.03508.x (2011).
79 Li, J. *et al.* Vascular risk factors promote conversion from mild cognitive impairment to Alzheimer disease. *Neurology* **76**, 1485-1491, doi:10.1212/WNL.0b013e318217e7a4 (2011).
80 Richardson, K. *et al.* The neuropathology of vascular disease in the Medical Research Council Cognitive Function and Ageing Study (MRC CFAS). *Curr Alzheimer Res* **9**, 687-696, doi:10.2174/156720512801322654 (2012).
81 Kynast, J. *et al.* White matter hyperintensities associated with small vessel disease impair social cognition beside attention and memory. *J Cereb Blood Flow Metab* **38**, 996-1009, doi:10.1177/0271678X17719380 (2018).
82 Thrift, A. G., Dewey, H. M., Macdonell, R. A., McNeil, J. J. & Donnan, G. A. Incidence of the major stroke subtypes: initial findings from the North East Melbourne stroke incidence study (NEMESIS). *Stroke* **32**, 1732-1738, doi:10.1161/01.str.32.8.1732 (2001).
83 Bejot, Y. *et al.* One-year survival of demented stroke patients: data from the Dijon Stroke Registry, France (1985-2008). *Eur J Neurol* **19**, 712-717, doi:10.1111/j.1468-1331.2011.03613.x (2012).
84 Thomalla, G., Glauche, V., Weiller, C. & Rother, J. Time course of wallerian degeneration after ischaemic stroke revealed by diffusion tensor imaging. *J Neurol Neurosurg Psychiatry* **76**, 266-268, doi:10.1136/jnnp.2004.046375 (2005).
85 Vonsattel, J. P. *et al.* Cerebral amyloid angiopathy without and with cerebral hemorrhages: a comparative histological study. *Ann Neurol* **30**, 637-649, doi:10.1002/ana.410300503 (1991).
86 Deramecourt, V. *et al.* Staging and natural history of cerebrovascular pathology in dementia. *Neurology* **78**, 1043-1050, doi:10.1212/WNL.0b013e31824e8e7f (2012).
87 Kalaria, R. N. *et al.* Towards defining the neuropathological substrates of vascular dementia. *J Neurol Sci* **226**, 75-80, doi:10.1016/j.jns.2004.09.019 (2004).
88 Strozyk, D. *et al.* Contribution of vascular pathology to the clinical expression of dementia. *Neurobiol Aging* **31**, 1710-1720, doi:10.1016/j.neurobiolaging.2008.09.011 (2010).
89 Blevins, B. L. *et al.* Brain arteriolosclerosis. *Acta Neuropathol* **141**, 1-24, doi:10.1007/s00401-020-02235-6 (2021).
90 Brun, A. & Englund, E. A white matter disorder in dementia of the Alzheimer type: a pathoanatomical study. *Ann Neurol* **19**, 253-262, doi:10.1002/ana.410190306 (1986).
91 Jellinger, K. A. & Attems, J. Incidence of cerebrovascular lesions in Alzheimer's disease: a postmortem study. *Acta Neuropathol* **105**, 14-17, doi:10.1007/s00401-002-0634-5 (2003).
92 Aue, W. P., Bartholdi, E. & Ernst, R. R. Two-dimensional spectroscopy. Application to nuclear magnetic resonance. *The Journal of Chemical Physics* **64**, 2229-2246, doi:10.1063/1.432450 (1976).
93 Tkac, I. *et al.* Highly resolved in vivo 1H NMR spectroscopy of the mouse brain at 9.4 T. *Magn Reson Med* **52**, 478-484, doi:10.1002/mrm.20184 (2004).
94 Nicholas, P. C., Kim, D., Crews, F. T. & Macdonald, J. M. 1H NMR-based metabolomic analysis of liver, serum, and brain following ethanol administration in rats. *Chem Res Toxicol* **21**, 408-420, doi:10.1021/tx700324t (2008).
95 Mahajan, U. V. *et al.* Dysregulation of multiple metabolic networks related to brain transmethylation and polyamine pathways in Alzheimer disease: A targeted metabolomic and transcriptomic study. *PLoS Med* **17**, e1003012, doi:10.1371/journal.pmed.1003012 (2020).

96 Lust, W. D., Passonneau, J. V. & Veech, R. L. Cyclic adenosine monphosphate, metabolites, and phosphorylase in neural tissue: a comparison a methods of fixation. *Science* **181**, 280-282, doi:10.1126/science.181.4096.280 (1973).
97 Medina, M. A., Jones, D. J., Stavinoha, W. B. & Ross, D. H. The levels of labile intermediary metabolites in mouse brain following rapid tissue fixation with microwave irradiation. *J Neurochem* **24**, 223-227, doi:10.1111/j.1471-4159.1975.tb11868.x (1975).
98 Veech, R. L., Harris, R. L., Veloso, D. & Veech, E. H. Freeze-blowing: a new technique for the study of brain in vivo. *J Neurochem* **20**, 183-188, doi:10.1111/j.1471-4159.1973.tb12115.x (1973).
99 Farias, S. E. *et al.* Formation of eicosanoids, E2/D2 isoprostanes, and docosanoids following decapitation-induced ischemia, measured in high-energy-microwaved rat brain. *J Lipid Res* **49**, 1990-2000, doi:10.1194/jlr.M800200-JLR200 (2008).
100 Ramadan, E. *et al.* Extracellular-derived calcium does not initiate in vivo neurotransmission involving docosahexaenoic acid. *J Lipid Res* **51**, 2334-2340, doi:10.1194/jlr.M006262 (2010).
101 Hennebelle, M. *et al.* Brain oxylipin concentrations following hypercapnia/ischemia: effects of brain dissection and dissection time. *J Lipid Res* **60**, 671-682, doi:10.1194/jlr.D084228 (2019).
102 Golovko, M. Y. & Murphy, E. J. An improved LC-MS/MS procedure for brain prostanoid analysis using brain fixation with head-focused microwave irradiation and liquid-liquid extraction. *J Lipid Res* **49**, 893-902, doi:10.1194/jlr.D700030-JLR200 (2008).
103 Richter, D. & Crossland, J. Variation in acetylcholine content of the brain with physiological state. *Am J Physiol* **159**, 247-255, doi:10.1152/ajplegacy.1949.159.2.247 (1949).
104 Takahashi, R. & Aprison, M. H. Acetylcholine Content of Discrete Areas of the Brain Obtained by a near-Freezing Method. *J Neurochem* **11**, 887-898, doi:10.1111/j.1471-4159.1964.tb06740.x (1964).
105 Hennebelle, M. *et al.* Linoleic acid participates in the response to ischemic brain injury through oxidized metabolites that regulate neurotransmission. *Sci Rep* **7**, 4342, doi:10.1038/s41598-017-02914-7 (2017).
106 Balcom, G. J., Lenox, R. H. & Meyerhoff, J. L. Regional glutamate levels in rat brain determined after microwave fixation. *J Neurochem* **26**, 423-425 (1976).
107 Balcom, G. J., Lenox, R. H. & Meyerhoff, J. L. Regional gamma-aminobutyric acid levels in rat brain determined after microwave fixation. *J Neurochem* **24**, 609-613 (1975).
108 Nihei, H., Kanemitsu, H., Tamura, A., Oka, H. & Sano, K. Cerebral uric acid, xanthine, and hypoxanthine after ischemia: the effect of allopurinol. *Neurosurgery* **25**, 613-617, doi:10.1097/00006123-198910000-00016 (1989).
109 Richter, J. A., Perry, E. K. & Tomlinson, B. E. Acetylcholine and choline levels in post-mortem human brain tissue: preliminary observations in Alzheimer's disease. *Life Sci* **26**, 1683-1689, doi:10.1016/0024-3205(80)90176-9 (1980).
110 Crossland, J. & Merrick, A. J. The effect of anaesthesia on the acetylcholine content of brain. *J Physiol* **125**, 56-66, doi:10.1113/jphysiol.1954.sp005142 (1954).
111 Schmidt, M. J., Schmidt, D. E. & Robison, G. A. Cyclic adenosine monophosphate in brain areas: microwave irradiation as a means of tissue fixation. *Science* **173**, 1142-1143 (1971).
112 Gonzalez-Riano, C. *et al.* Metabolic Changes in Brain Slices over Time: a Multiplatform Metabolomics Approach. *Mol Neurobiol* **58**, 3224-3237, doi:10.1007/s12035-020-02264-y (2021).
113 Folch, J., Lees, M. & Sloane Stanley, G. H. A simple method for the isolation and purification of total lipides from animal tissues. *J Biol Chem* **226**, 497-509 (1957).
114 O'Sullivan, A. *et al.* Metabolomics of cerebrospinal fluid from humans treated for rabies. *J Proteome Res* **12**, 481-490, doi:10.1021/pr3009176 (2013).

115 Sladojevic, N., Yu, B. & Liao, J. K. Regulator of G-Protein Signaling 5 Maintains Brain Endothelial Cell Function in Focal Cerebral Ischemia. *J Am Heart Assoc* **9**, e017533, doi:10.1161/JAHA.120.017533 (2020).
116 Nilsson, L., Kogure, K. & Busto, R. Effects of hypothermia and hyperthermia on brain energy metabolism. *Acta Anaesthesiol Scand* **19**, 199-205, doi:10.1111/j.1399-6576.1975.tb05241.x (1975).
117 Cullingford, T. E., Eagles, D. A. & Sato, H. The ketogenic diet upregulates expression of the gene encoding the key ketogenic enzyme mitochondrial 3-hydroxy-3-methylglutaryl-CoA synthase in rat brain. *Epilepsy Res* **49**, 99-107, doi:10.1016/s0920-1211(02)00011-6 (2002).
118 Cullingford, T. E. *et al.* Molecular cloning of rat mitochondrial 3-hydroxy-3-methylglutaryl-CoA lyase and detection of the corresponding mRNA and of those encoding the remaining enzymes comprising the ketogenic 3-hydroxy-3-methylglutaryl-CoA cycle in central nervous system of suckling rat. *Biochem J* **329 (Pt 2)**, 373-381, doi:10.1042/bj3290373 (1998).
119 Dienel, G. A. Brain lactate metabolism: the discoveries and the controversies. *J Cereb Blood Flow Metab* **32**, 1107-1138, doi:10.1038/jcbfm.2011.175 (2012).
120 Krebs, H. A. The citric acid cycle and the Szent-Gyorgyi cycle in pigeon breast muscle. *Biochem J* **34**, 775-779, doi:10.1042/bj0340775 (1940).
121 Faggi, L. *et al.* A Polyphenol-Enriched Supplement Exerts Potent Epigenetic-Protective Activity in a Cell-Based Model of Brain Ischemia. *Nutrients* **11**, doi:10.3390/nu11020345 (2019).
122 Kamphorst, J. J., Chung, M. K., Fan, J. & Rabinowitz, J. D. Quantitative analysis of acetyl-CoA production in hypoxic cancer cells reveals substantial contribution from acetate. *Cancer Metab* **2**, 23, doi:10.1186/2049-3002-2-23 (2014).
123 Walsh, J. L., Percival, A. & Turner, P. V. Efficacy of Blunt Force Trauma, a Novel Mechanical Cervical Dislocation Device, and a Non-Penetrating Captive Bolt Device for On-Farm Euthanasia of Pre-Weaned Kits, Growers, and Adult Commercial Meat Rabbits. *Animals (Basel)* **7**, doi:10.3390/ani7120100 (2017).
124 Greco, T., Vespa, P. M. & Prins, M. L. Alternative substrate metabolism depends on cerebral metabolic state following traumatic brain injury. *Exp Neurol* **329**, 113289, doi:10.1016/j.expneurol.2020.113289 (2020).
125 Lee, B. E. *et al.* O-GlcNAcylation regulates dopamine neuron function, survival and degeneration in Parkinson disease. *Brain* **143**, 3699-3716, doi:10.1093/brain/awaa320 (2020).
126 Stewart, L. T., Abiraman, K., Chatham, J. C. & McMahon, L. L. Increased O-GlcNAcylation rapidly decreases GABAAR currents in hippocampus but depresses neuronal output. *Sci Rep* **10**, 7494, doi:10.1038/s41598-020-63188-0 (2020).
127 Blaschko, H. The activity of l(-)-dopa decarboxylase. *J Physiol* **101**, 337-349, doi:10.1113/jphysiol.1942.sp003988 (1942).
128 Huger, F. & Patrick, G. Effect of concussive head injury on central catecholamine levels and synthesis rates in rat brain regions. *J Neurochem* **33**, 89-95, doi:10.1111/j.1471-4159.1979.tb11710.x (1979).
129 Bazan, N. G., Jr. Effects of ischemia and electroconvulsive shock on free fatty acid pool in the brain. *Biochim Biophys Acta* **218**, 1-10, doi:10.1016/0005-2760(70)90086-x (1970).
130 Horowitz, H. H., Doerschuk, A. P. & King, C. G. [The origin of L-ascorbic acid in the albino rat]. *J Biol Chem* **199**, 193-198 (1952).
131 Miura, S. *et al.* Ascorbic acid protects the newborn rat brain from hypoxic-ischemia. *Brain Dev* **31**, 307-317, doi:10.1016/j.braindev.2008.06.010 (2009).
132 Kahl, A. *et al.* Critical Role of Flavin and Glutathione in Complex I-Mediated Bioenergetic Failure in Brain Ischemia/Reperfusion Injury. *Stroke* **49**, 1223-1231, doi:10.1161/STROKEAHA.117.019687 (2018).

133 Desole, M. S. *et al.* The effects of cortical ablation on d-amphetamine-induced changes in striatal dopamine turnover and ascorbic acid catabolism in the rat. *Neurosci Lett* **139**, 29-33, doi:10.1016/0304-3940(92)90850-7 (1992).
134 Lowry, O. H., Rosebrough, N. J., Farr, A. L. & Randall, R. J. Protein measurement with the Folin phenol reagent. *J Biol Chem* **193**, 265-275 (1951).
135 Burns, A. & Iliffe, S. Dementia. *BMJ* **338**, b75, doi:10.1136/bmj.b75 (2009).
136 Cummings, J. L., Tong, G. & Ballard, C. Treatment Combinations for Alzheimer's Disease: Current and Future Pharmacotherapy Options. *J Alzheimers Dis* **67**, 779-794, doi:10.3233/JAD-180766 (2019).
137 Gootjes, L. *et al.* Regional distribution of white matter hyperintensities in vascular dementia, Alzheimer's disease and healthy aging. *Dement Geriatr Cogn Disord* **18**, 180-188, doi:10.1159/000079199 (2004).
138 Barber, R. *et al.* White matter lesions on magnetic resonance imaging in dementia with Lewy bodies, Alzheimer's disease, vascular dementia, and normal aging. *J Neurol Neurosurg Psychiatry* **67**, 66-72, doi:10.1136/jnnp.67.1.66 (1999).
139 Toledo, J. B. *et al.* Contribution of cerebrovascular disease in autopsy confirmed neurodegenerative disease cases in the National Alzheimer's Coordinating Centre. *Brain* **136**, 2697-2706, doi:10.1093/brain/awt188 (2013).
140 Fleisher, A. S. *et al.* Positron Emission Tomography Imaging With [18F]flortaucipir and Postmortem Assessment of Alzheimer Disease Neuropathologic Changes. *JAMA Neurol*, doi:10.1001/jamaneurol.2020.0528 (2020).
141 Graham, S. F., Holscher, C. & Green, B. D. Metabolic signatures of human Alzheimer's disease (AD): 1H NMR analysis of the polar metabolome of post-mortem brain tissue. *Metabolomics* **10**, 744-753, doi:10.1007/s11306-013-0610-1 (2014).
142 Kim, Y. H. *et al.* Metabolomic Analysis Identifies Alterations of Amino Acid Metabolome Signatures in the Postmortem Brain of Alzheimer's Disease. *Exp Neurobiol* **28**, 376-389, doi:10.5607/en.2019.28.3.376 (2019).
143 Corder, E. H. *et al.* Gene dose of apolipoprotein E type 4 allele and the risk of Alzheimer's disease in late onset families. *Science* **261**, 921-923, doi:10.1126/science.8346443 (1993).
144 Czapiga, M. & Colton, C. A. Microglial function in human APOE3 and APOE4 transgenic mice: altered arginine transport. *J Neuroimmunol* **134**, 44-51, doi:10.1016/s0165-5728(02)00394-6 (2003).
145 Hibbs, J. B., Jr., Vavrin, Z. & Taintor, R. R. L-arginine is required for expression of the activated macrophage effector mechanism causing selective metabolic inhibition in target cells. *J Immunol* **138**, 550-565 (1987).
146 Le Douce, J. *et al.* Impairment of Glycolysis-Derived l-Serine Production in Astrocytes Contributes to Cognitive Deficits in Alzheimer's Disease. *Cell Metab* **31**, 503-517 e508, doi:10.1016/j.cmet.2020.02.004 (2020).
147 Bergin, D. H. *et al.* Altered plasma arginine metabolome precedes behavioural and brain arginine metabolomic profile changes in the APPswe/PS1DeltaE9 mouse model of Alzheimer's disease. *Transl Psychiatry* **8**, 108, doi:10.1038/s41398-018-0149-z (2018).
148 Otoki, Y. *et al.* Lipidomic Analysis of Postmortem Prefrontal Cortex Phospholipids Reveals Changes in Choline Plasmalogen Containing Docosahexaenoic Acid and Stearic Acid Between Cases With and Without Alzheimer's Disease. *Neuromolecular Med* **23**, 161-175, doi:10.1007/s12017-020-08636-w (2021).
149 Hyman, B. T. *et al.* National Institute on Aging-Alzheimer's Association guidelines for the neuropathologic assessment of Alzheimer's disease. *Alzheimers Dement* **8**, 1-13, doi:10.1016/j.jalz.2011.10.007 (2012).

150 Mandal, P. K., Saharan, S., Tripathi, M. & Murari, G. Brain glutathione levels--a novel biomarker for mild cognitive impairment and Alzheimer's disease. *Biol Psychiatry* **78**, 702-710, doi:10.1016/j.biopsych.2015.04.005 (2015).
151 Mandal, P. K., Tripathi, M. & Sugunan, S. Brain oxidative stress: detection and mapping of anti-oxidant marker 'Glutathione' in different brain regions of healthy male/female, MCI and Alzheimer patients using non-invasive magnetic resonance spectroscopy. *Biochem Biophys Res Commun* **417**, 43-48, doi:10.1016/j.bbrc.2011.11.047 (2012).
152 Hodgson, N., Trivedi, M., Muratore, C., Li, S. & Deth, R. Soluble oligomers of amyloid-beta cause changes in redox state, DNA methylation, and gene transcription by inhibiting EAAT3 mediated cysteine uptake. *J Alzheimers Dis* **36**, 197-209, doi:10.3233/JAD-130101 (2013).
153 Huang, W. J., Zhang, X. & Chen, W. W. Role of oxidative stress in Alzheimer's disease. *Biomed Rep* **4**, 519-522, doi:10.3892/br.2016.630 (2016).
154 Blumenstein, J. & Williams, G. R. Glycine methyltransferase. *Can J Biochem Physiol* **41**, 201-210 (1963).
155 Garrow, T. A. Purification, kinetic properties, and cDNA cloning of mammalian betaine-homocysteine methyltransferase. *J Biol Chem* **271**, 22831-22838, doi:10.1074/jbc.271.37.22831 (1996).
156 Lehmann, M., Gottfries, C. G. & Regland, B. Identification of cognitive impairment in the elderly: homocysteine is an early marker. *Dement Geriatr Cogn Disord* **10**, 12-20, doi:10.1159/000017092 (1999).
157 Rossi, A. *et al.* Defective Mitochondrial Pyruvate Flux Affects Cell Bioenergetics in Alzheimer's Disease-Related Models. *Cell Rep* **30**, 2332-2348 e2310, doi:10.1016/j.celrep.2020.01.060 (2020).
158 Yao, J. *et al.* Mitochondrial bioenergetic deficit precedes Alzheimer's pathology in female mouse model of Alzheimer's disease. *Proc Natl Acad Sci U S A* **106**, 14670-14675, doi:10.1073/pnas.0903563106 (2009).
159 Mazaheri, F. *et al.* TREM2 deficiency impairs chemotaxis and microglial responses to neuronal injury. *EMBO Rep* **18**, 1186-1198, doi:10.15252/embr.201743922 (2017).
160 Sarajas, H. S. & Oja, S. S. Effect of anesthesia and-or hypothermia on cerebral free amino acids in young rats. *Dev Psychobiol* **6**, 385-392, doi:10.1002/dev.420060502 (1973).
161 Rosomoff, H. L. & Holaday, D. A. Cerebral blood flow and cerebral oxygen consumption during hypothermia. *Am J Physiol* **179**, 85-88, doi:10.1152/ajplegacy.1954.179.1.85 (1954).
162 Shapiro, H. A. The post-mortem temperature plateau. *J Forensic Med* **12**, 137-141 (1965).
163 Schoenmackers, J. [Optimal refrigeration for cadavers and equipment of cooling rooms]. *Zentralbl Allg Pathol* **96**, 280-286 (1957).
164 Anton, R. F., Wallis, C. & Randall, C. L. In vivo regional levels of PGE and thromboxane in mouse brain: effect of decapitation, focused microwave fixation, and indomethacin. *Prostaglandins* **26**, 421-429, doi:10.1016/0090-6980(83)90177-6 (1983).
165 Deutsch, J., Rapoport, S. I. & Purdon, A. D. Relation between free fatty acid and acyl-CoA concentrations in rat brain following decapitation. *Neurochem Res* **22**, 759-765, doi:10.1023/a:1022030306359 (1997).
166 Golovko, M. Y. & Murphy, E. J. Brain prostaglandin formation is increased by alpha-synuclein gene-ablation during global ischemia. *Neurosci Lett* **432**, 243-247, doi:10.1016/j.neulet.2007.12.031 (2008).
167 Murphy, E. J. Brain fixation for analysis of brain lipid-mediators of signal transduction and brain eicosanoids requires head-focused microwave irradiation: an historical perspective. *Prostaglandins Other Lipid Mediat* **91**, 63-67, doi:10.1016/j.prostaglandins.2009.07.005 (2010).

168 Savaki, H. E., Davidsen, L., Smith, C. & Sokoloff, L. Measurement of free glucose turnover in brain. *J Neurochem* **35**, 495-502, doi:10.1111/j.1471-4159.1980.tb06293.x (1980).
169 Phelps, M. E. *et al.* Tomographic measurement of local cerebral glucose metabolic rate in humans with (F-18)2-fluoro-2-deoxy-D-glucose: validation of method. *Ann Neurol* **6**, 371-388, doi:10.1002/ana.410060502 (1979).
170 Reivich, M. *et al.* Use of 2-deoxy-D[1-11C]glucose for the determination of local cerebral glucose metabolism in humans: variation within and between subjects. *J Cereb Blood Flow Metab* **2**, 307-319, doi:10.1038/jcbfm.1982.32 (1982).
171 DeMar, J. C., Jr., Ma, K., Bell, J. M. & Rapoport, S. I. Half-lives of docosahexaenoic acid in rat brain phospholipids are prolonged by 15 weeks of nutritional deprivation of n-3 polyunsaturated fatty acids. *J Neurochem* **91**, 1125-1137, doi:10.1111/j.1471-4159.2004.02789.x (2004).
172 Umhau, J. C. *et al.* Imaging incorporation of circulating docosahexaenoic acid into the human brain using positron emission tomography. *J Lipid Res* **50**, 1259-1268, doi:10.1194/jlr.M800530-JLR200 (2009).
173 Pichika, R. *et al.* The synthesis and in vivo pharmacokinetics of fluorinated arachidonic acid: implications for imaging neuroinflammation. *J Nucl Med* **53**, 1383-1391, doi:10.2967/jnumed.112.105734 (2012).